ELECTRONIC SUPPLEMENTARY INFORMATION

[1_4]Heterophane prototypes containing azolium and/or azole anion-binding motifs

Neus Mesquida,* Immaculada Dinarès, Anna Ibáñez and Ermitas Alcalde*
Laboratori de Química Orgànica, Facultat de Farmàcia, Universitat de Barcelona
Avda. Joan XXIII, s/n. 08028-Barcelona (Spain). E-mail:neusmesquida@ub.edu, ealcalde@ub.edu

Table of Contents

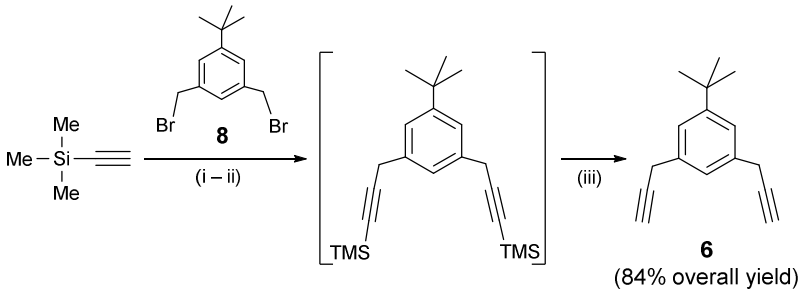

Scheme S1 Synthesis of dialkyne **6**: (i) *i*-PrMgCl, THF, 0 °C to rt, 1 h; (ii) CuBr, dibromide **8**, THF, reflux, 5 h; (iii) TBAF·H_2O, AcOH, THF, rt, 18 h.

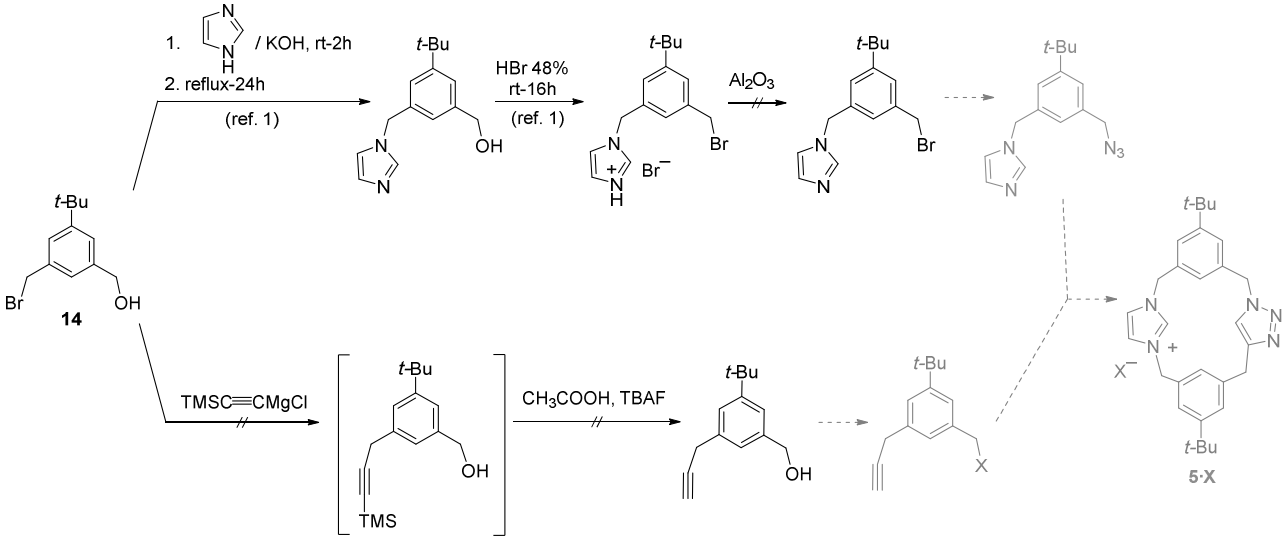

Scheme S2 Attempted synthesis of macrocycle **5·X**.

(*Ref. 1* Alcalde, E.; Ayala, C.; Dinarès, I.; Mesquida, N. *J. Org. Chem*, **2001**, *66*, 2291–2295)

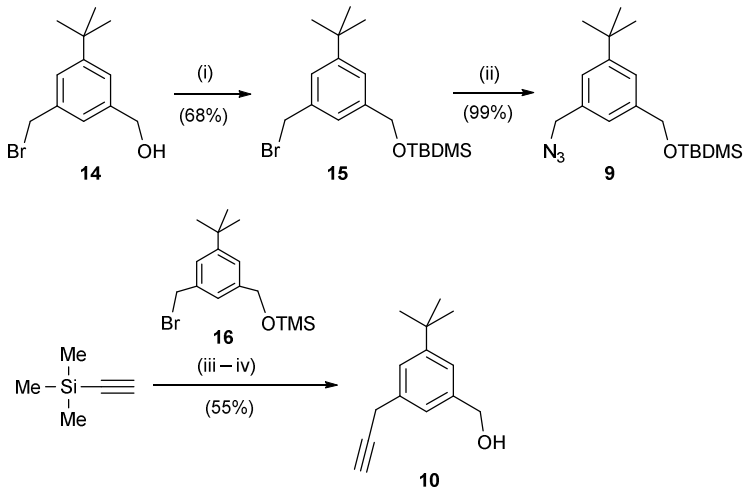

Scheme S3 Synthesis of azide **9** and alkyne **10**: (i) DIPEA, TBDMSCl, CH_2Cl_2, 0 °C to rt, 18 h; (ii) NaN_3, DMF, 60 °C; (vii) *i*-PrMgCl, THF, 0 °C to rt, 1 h; (iii) CuBr, bromide **16**, THF, reflux, 5 h; (iv) TBAF·H_2O, AcOH, THF, rt, 18 h. TBDMS: (*tert*-butyl)dimethylsilyl group.

NMR SPECTRA AND ESI(+)-HRMS SPECTRA OF MACROCYCLES 3, 4·2Cl AND 5·Cl

• [1$_4$]Triazolophane 3

^{1}H NMR (400 MHz, $CDCl_3$)

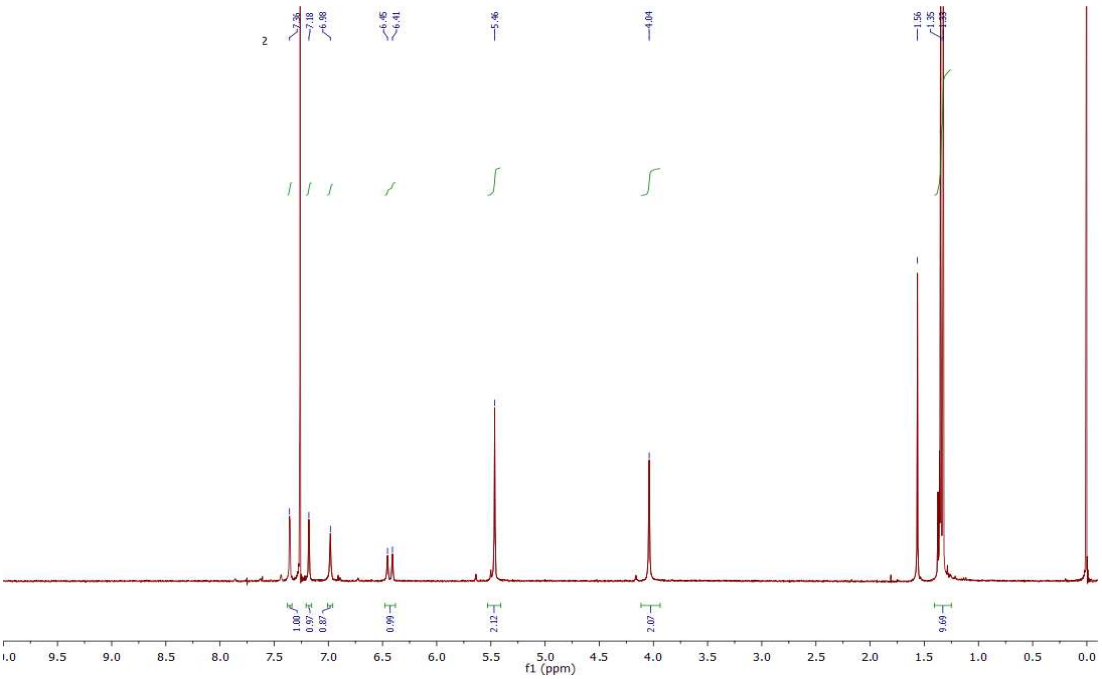

1D-NOESY experiment ($CDCl_3$)

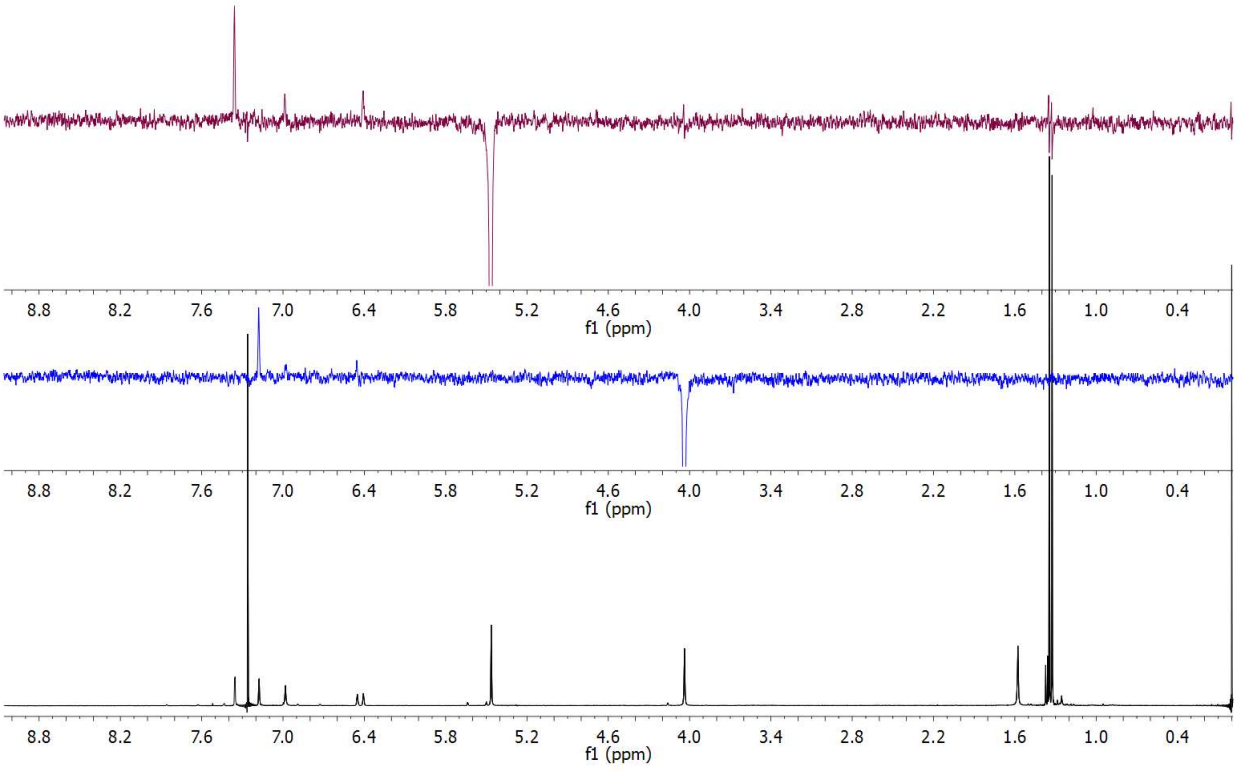

1D-NOESY experiment (DMSO-d_6)

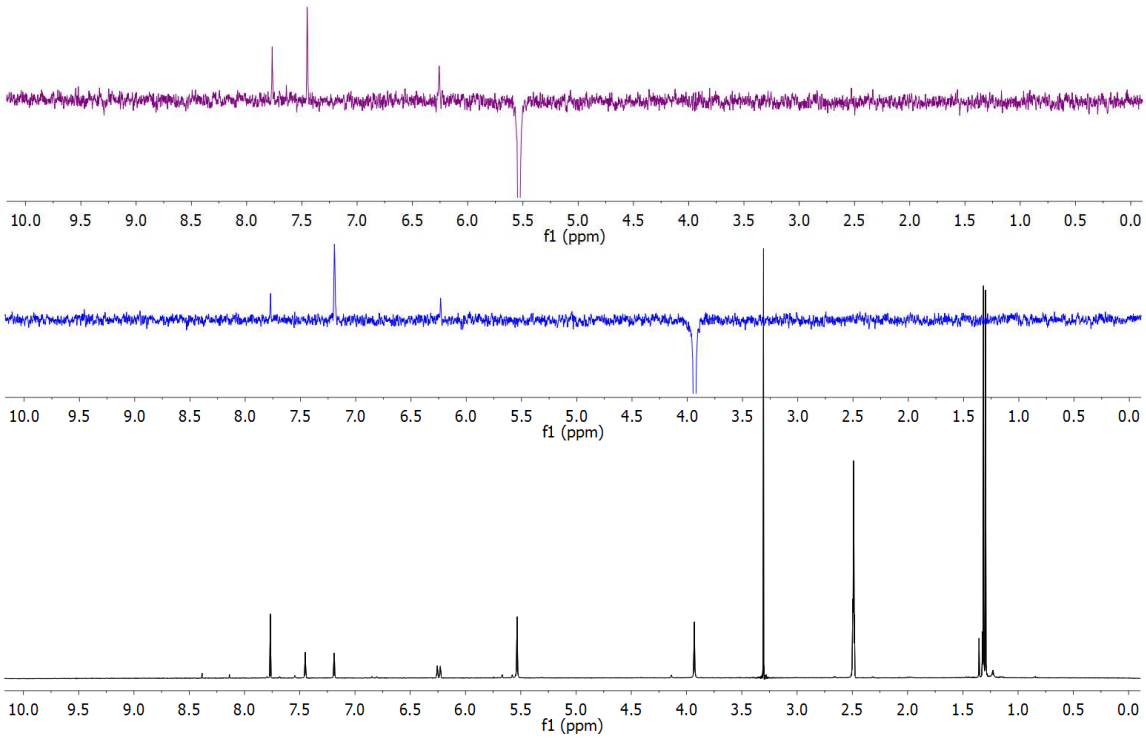

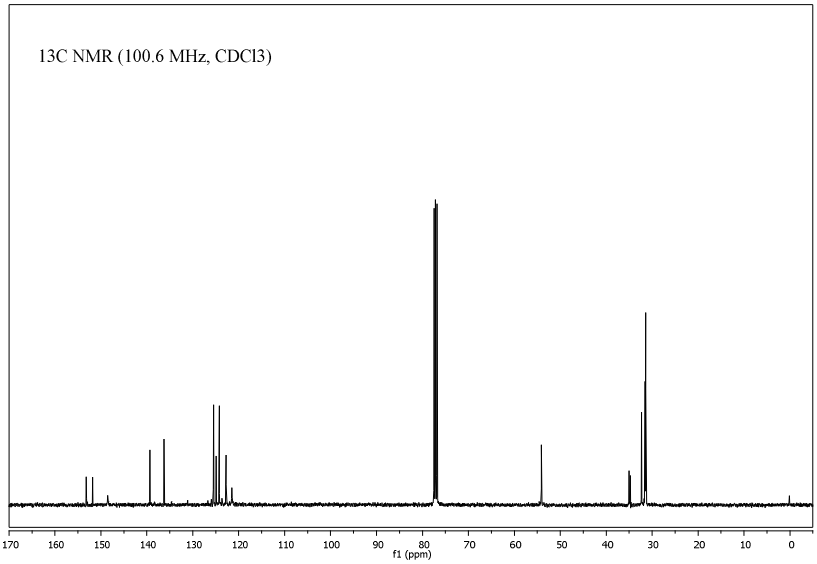

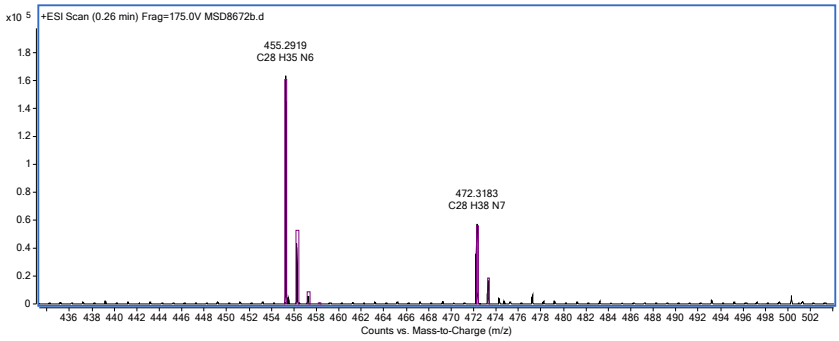

• **[1$_4$]Triazoliophane 4·2Cl**

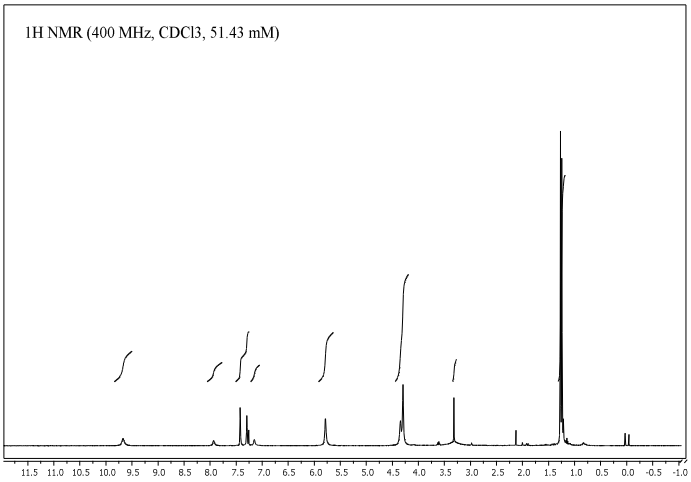

1D-NOESY experiment (DMSO-d$_6$)

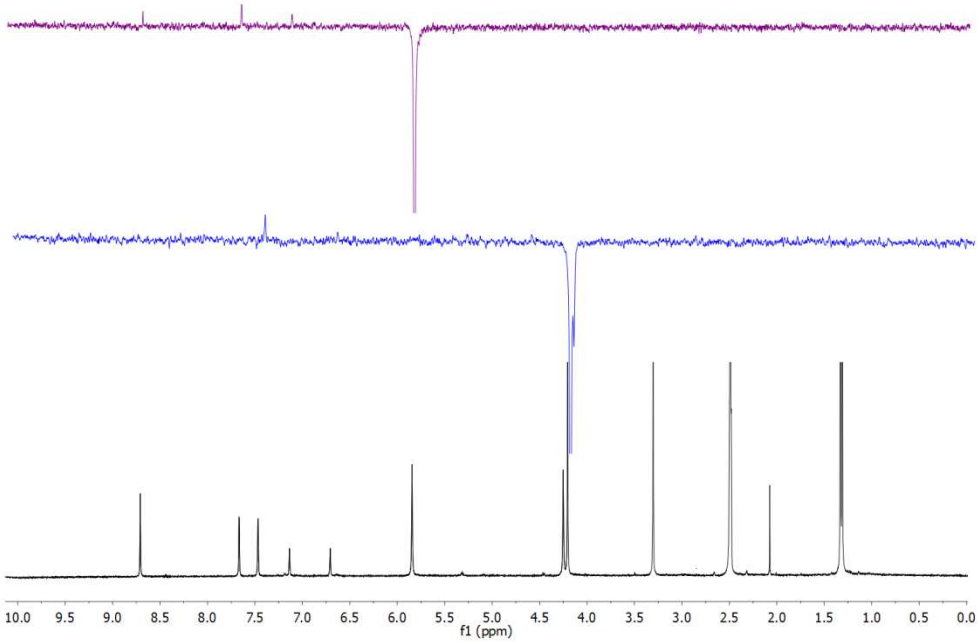

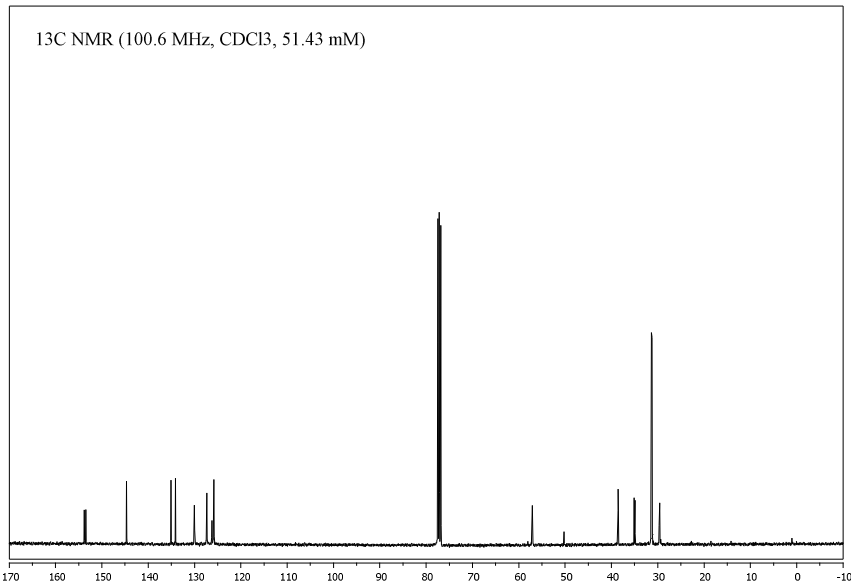

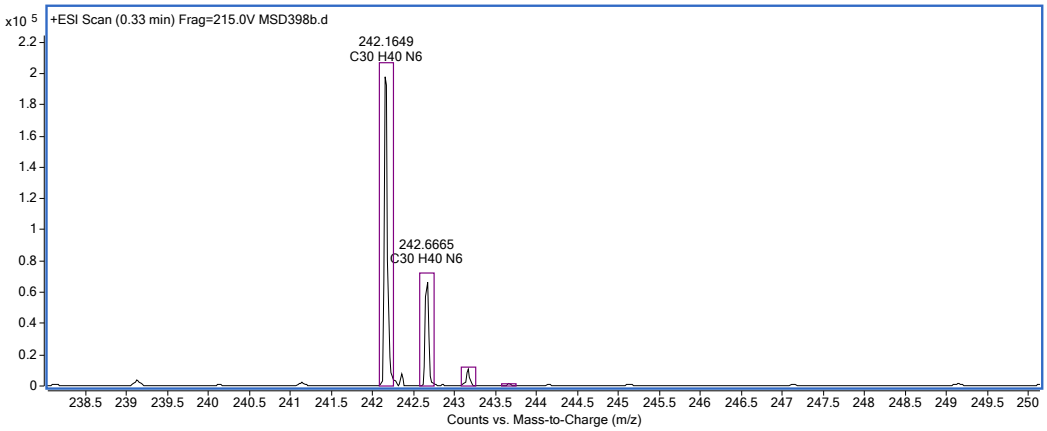

• Hybrid [1_4]heterophane 5·Cl

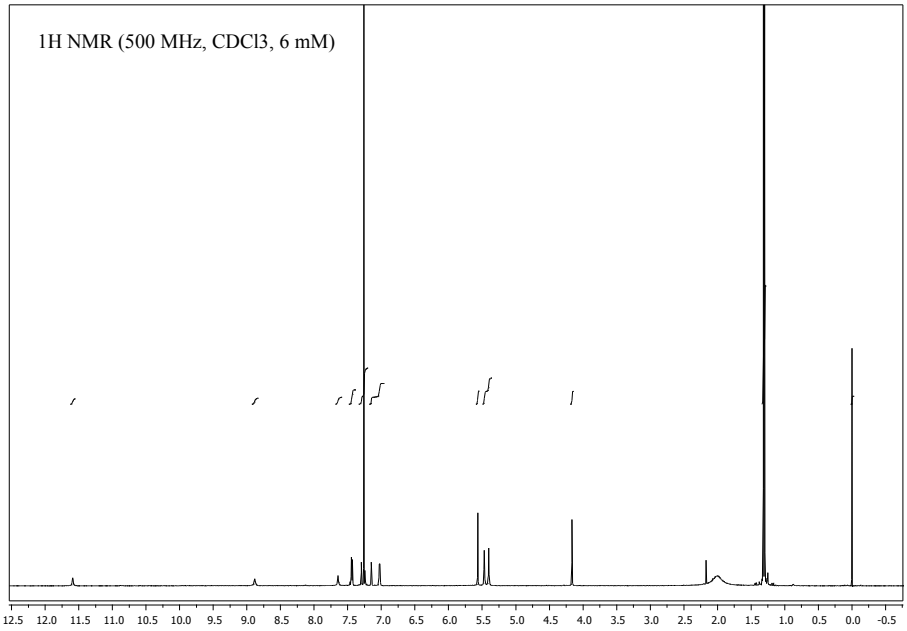

ROESY experiment ($CDCl_3$)

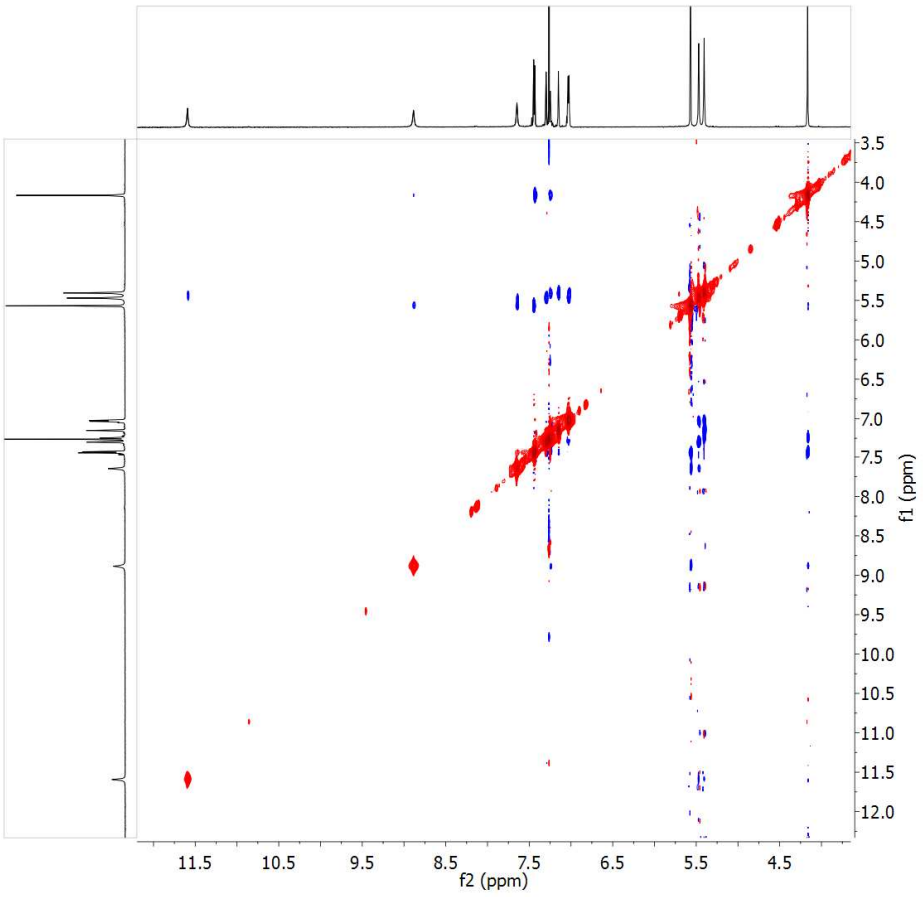

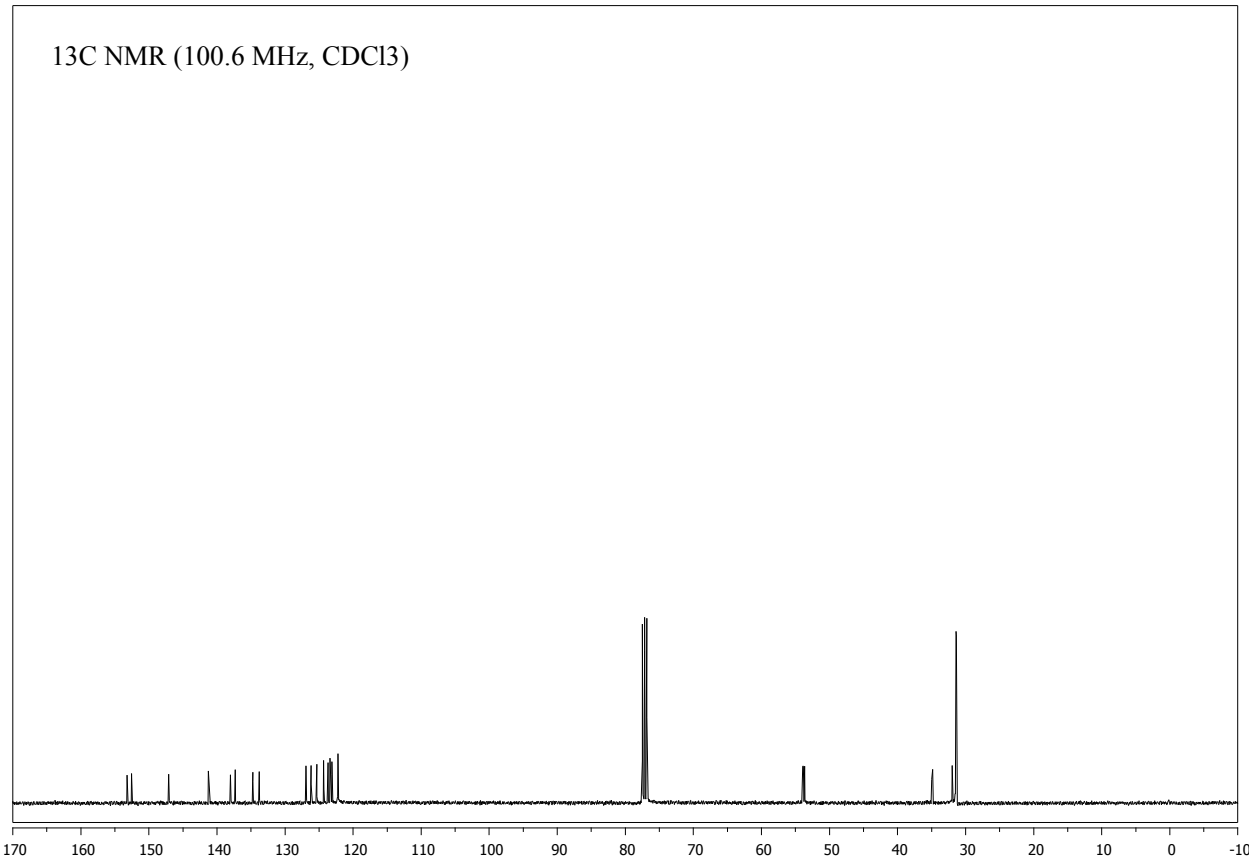

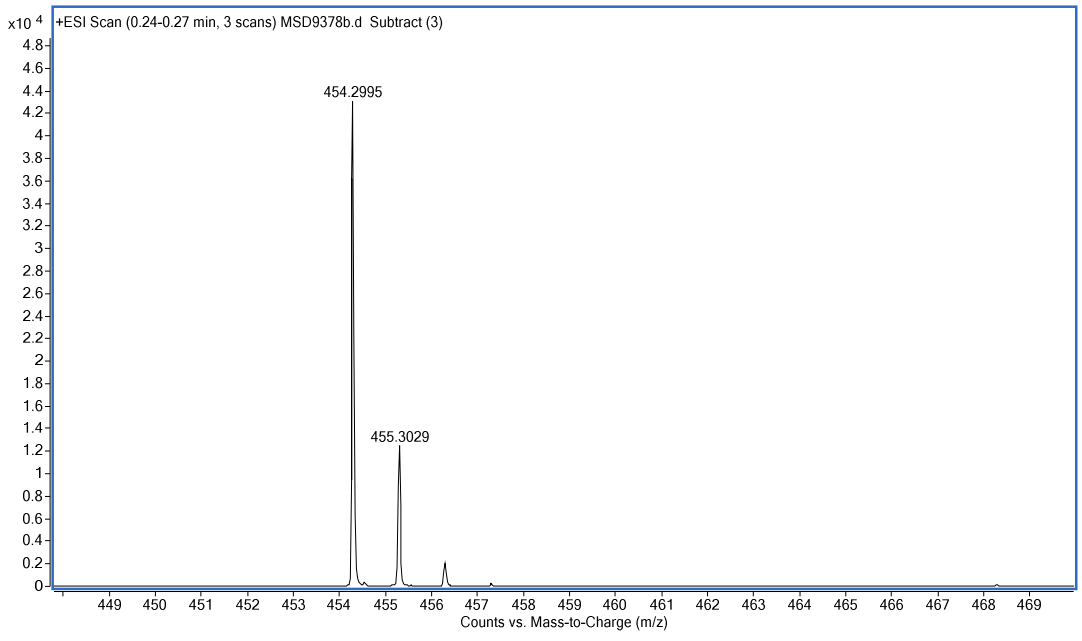

Table S1. Selected ^{1}H NMR (300 MHz, DMSO-d_6) spectroscopic data for [1_4]cyclophanes **1·2A**–**5·A** at 0.003 M.

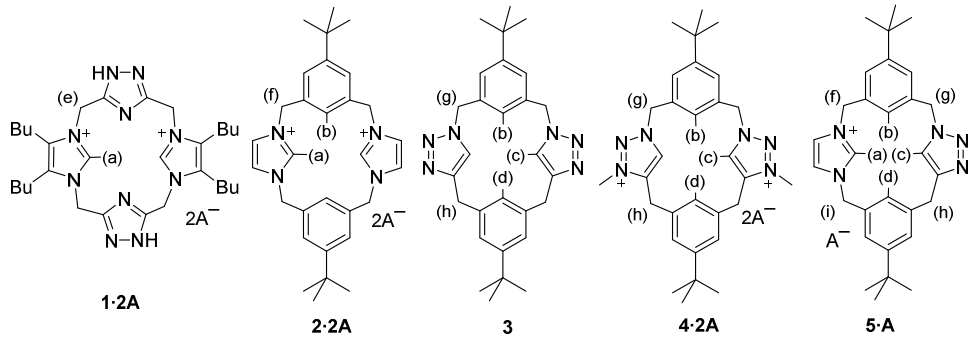

Compd.	H(a)	H(b)	H(c)	H(d)	CH_2(e)	CH_2(f)	CH_2(g)	CH_2(h)	CH_2(i)
1·2Cl	9.03	—	—	—	5.56	—	—	—	—
1·2AcO	8.89	—	—	—	5.42	—	—	—	—
1·2PF$_6$	9.00	—	—	—	5.52	—	—	—	—
2·2Br	9.37	6.70	—	—	—	5.43	—	—	—
2·2Cl	9.48	6.81	—	—	—	5.42	—	—	—
2·2AcO	10.37	7.31	—	—	—	5.39	—	—	—
2·2H$_2$PO$_4$	10.85	7.88	—	—	—	5.39	—	—	—
2·2PF$_6$	9.28	6.62	—	—	—	5.42	—	—	—
3[a,b]	—	6.26	7.76	6.23	—	—	5.53	3.93	—
3[a,b,c]	—	6.41	6.98	6.45	—	—	5.46	4.04	—
4·2Cl[b]	—	7.14	8.71	6.70	—	—	5.84	4.25	—
4·2PF$_6$	—	7.08	8.60	6.66	—	—	5.84	4.25	—
5·Cl	9.35	6.35	7.84	6.33	—	5.39	5.60	4.01	5.37
5·PF$_6$	9.32	6.31	7.83	6.33	—	5.38	5.60	4.01	5.37
5·PF$_6$[c]	8.81	6.49	7.72	6.56	—	5.29	5.53	4.09	5.26

[a] At 0.005 mM. [b] Unambiguous assignments were made by 1D-NOESY (400 MHz).
[c] In $CDCl_3$. [d] Unambiguous assignments were made by ROESY (500 MHz).

Table S2. Selected ^{1}H NMR (300 MHz) chemical shift values of compounds **1·2A**–**5·A** in DMSO-d_6, CD_3CN or $CDCl_3$ at 0.003 M.

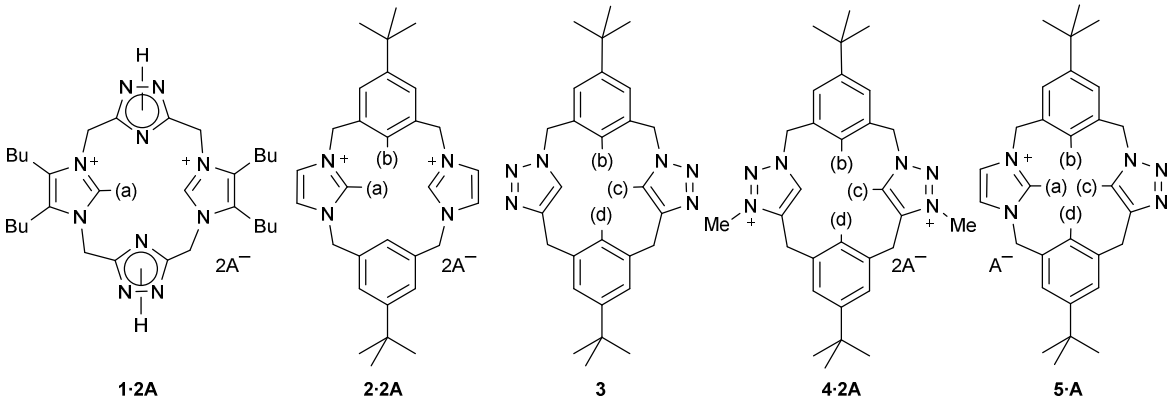

1·2A **2·2A** **3** **4·2A** **5·A**

Compd	Anion	DMSO-d_6				CD_3CN				$CDCl_3$			
		H(a)	H(b)	H(c)	H(d)	H(a)	H(b)	H(c)	H(d)	H(a)	H(b)	H(c)	H(d)
1·2A[a,b]	Cl^-	9.03	—	—	—								
	PF_6^-	9.00	—	—	—								
	Δδ[c]	0.03											
	AcO^-	8.89	—	—	—								
	Δδ[d]	–0.11											
2·2A[b]	Cl^-	9.48	6.81	—	—	11.00	8.46	—	—				
	PF_6^-[e]	9.28	6.62	—	—	8.35	6.51	—	—				
	Δδ[c]	0.20	0.19			2.65	1.95						
	AcO^-	10.37	7.31	—	—	11.43	8.15	—	—				
	Δδ[d]	1.09	0.69			3.08	1.64						
	$H_2PO_4^-$[a]	10.85	7.88	—	—								
	Δδ[f]	1.57	1.26										
3[a,e]		—	6.26	7.76	6.23					—	6.41	6.98	6.45
4·2A	Cl^-	—	7.14	8.71	6.70	—	7.73	9.23	7.16	—	7.84	10.01	7.26
	PF_6^-[e]	—	7.08	8.60	6.66	—	6.71	7.80	6.45	—	7.03	7.90	6.99
	Δδ[c]		0.06	0.11	0.03		1.02	1.43	0.71		0.81	2.11	0.27
5·A	Cl^-	9.35	6.35	7.84	6.33	9.27	6.78	7.84	6.71	11.67	7.47	8.62	7.39
	PF_6^-[e]	9.32	6.31	7.83	6.33	8.37	6.33	7.41	6.36	8.81	6.49	7.72	6.56
	Δδ[c]	0.03	0.04	0.01	0.00	0.90	0.45	0.43	0.35	2.86	0.98	0.90	0.83

[a]Not soluble in CD_3CN at 0.003M. [b]Not soluble in $CDCl_3$ at 0.003M. [c]Δδ, observed chemical shift difference between Cl^- salt and the corresponding PF_6^- salt. [d]Δδ, observed chemical shift difference between AcO^- salt and the corresponding PF_6^- salt. [e]Not soluble in D_2O at 0.003M. [f]Δδ, observed chemical shift difference between $H_2PO_4^-$ salt and the corresponding PF_6^- salt.

Figure S1. ^{1}H NMR spectra (low-field region) of heterophane **3** upon addition of increasing amounts of TBA·Cl (300MHz, 298 K) ***a)*** in $CDCl_3$, ***b)*** in DMSO-d_6.

a)

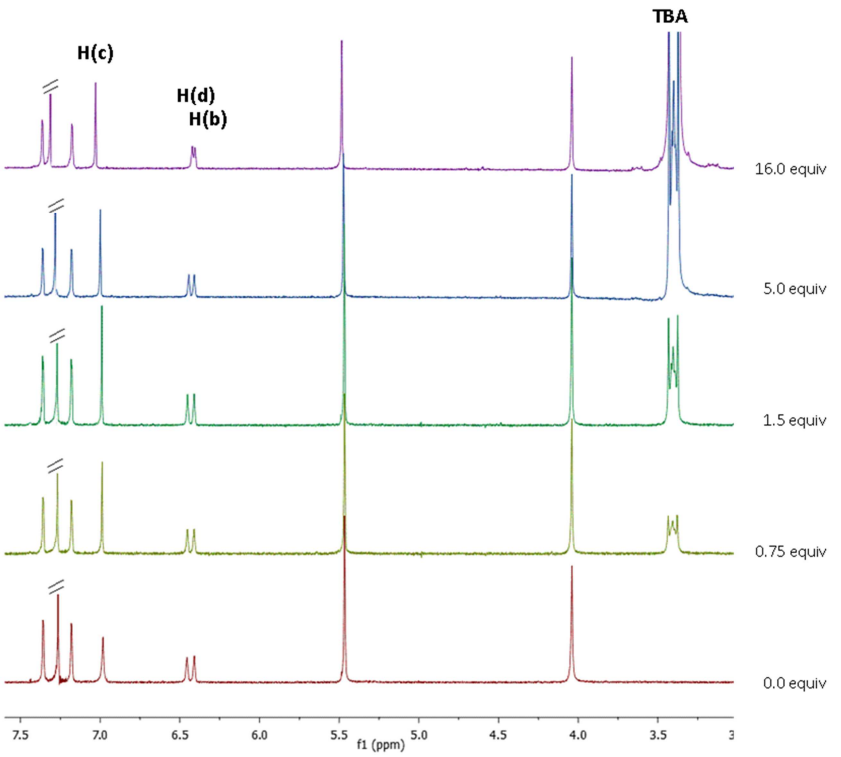

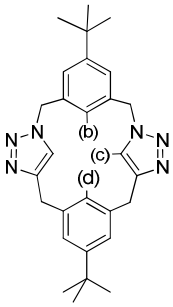

3

b)

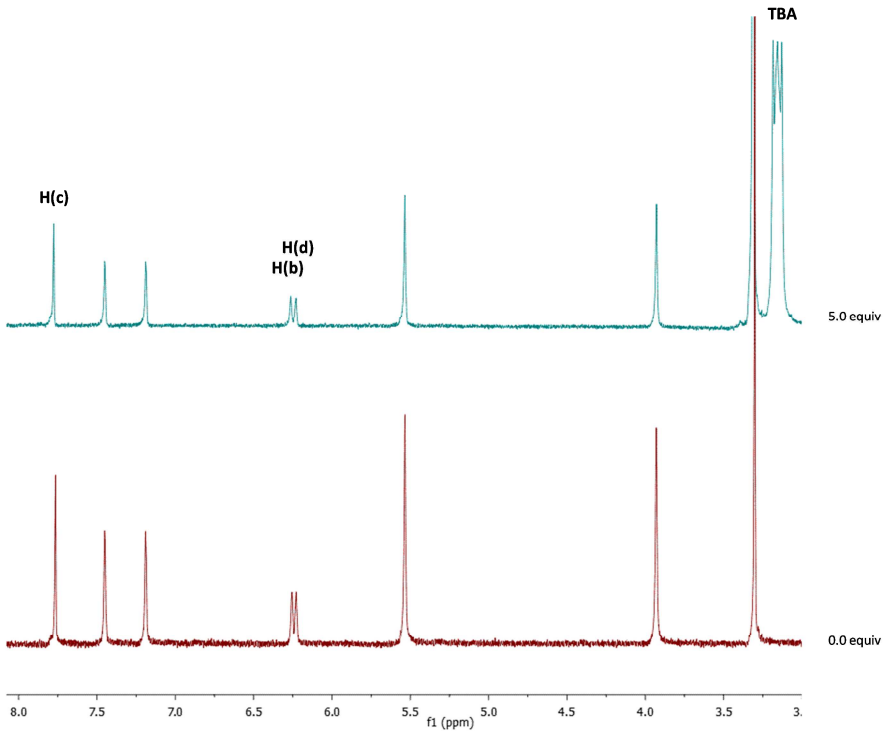

Figure S2. ^{1}H NMR spectra (low-field region) of heterophane **3** in $CDCl_3$ upon addition of increasing amounts of TBA·AcO (300MHz, 298 K).

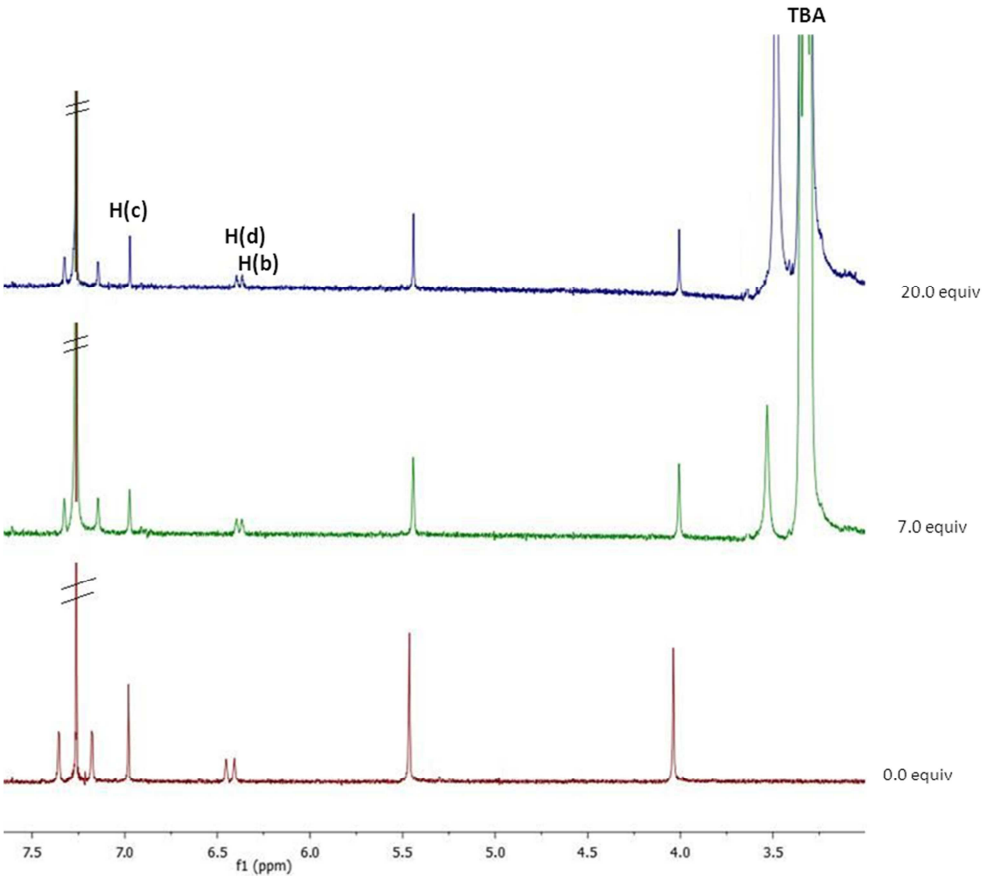

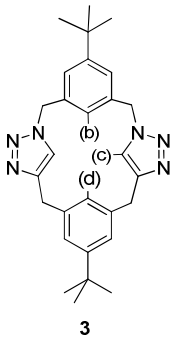

3

Figure S3. a) ^{1}H NMR (300MHz, 298K) spectra (low-field region) of receptor **2·2PF$_6$** in CD_3CN upon addition of increasing amounts of TBA·Cl (from bottom to top).
b) Job's plot representation from values of H(a) or H(b).

a)

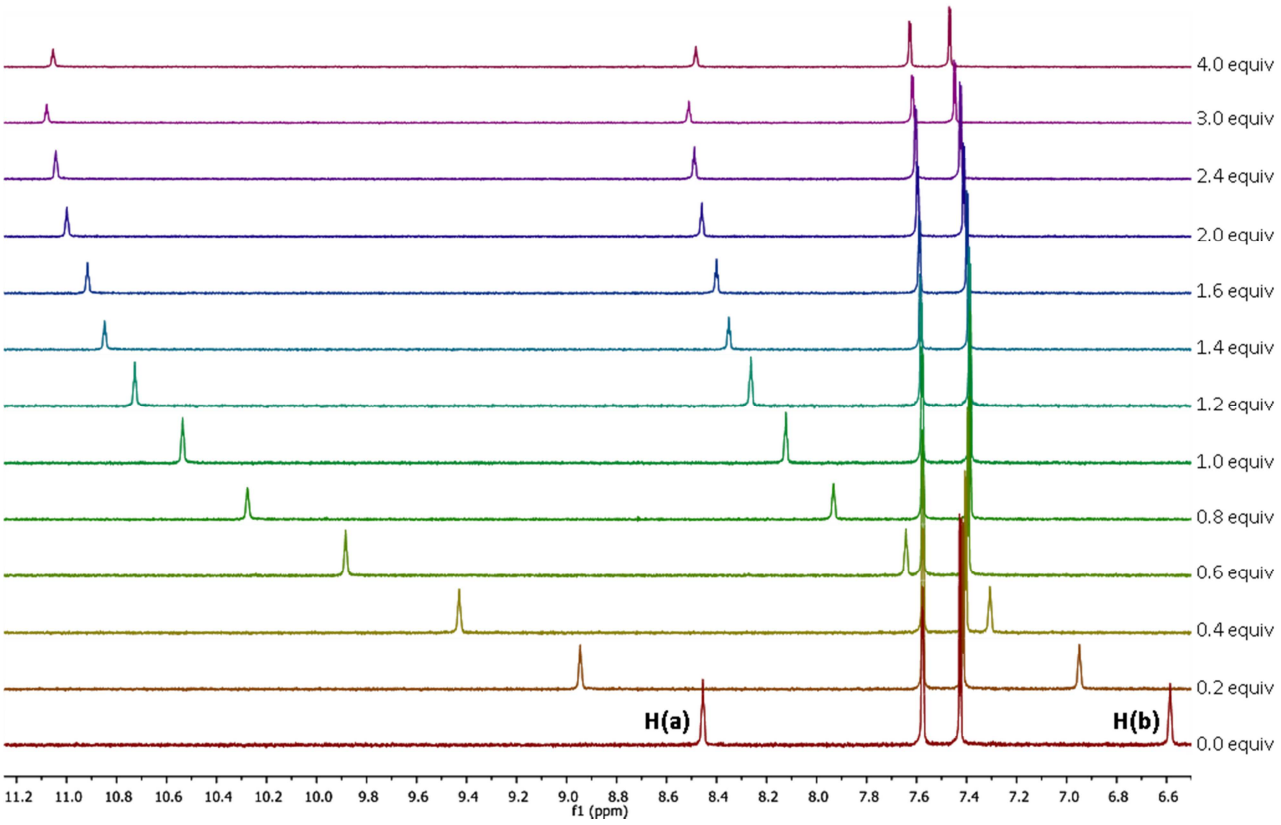

b)

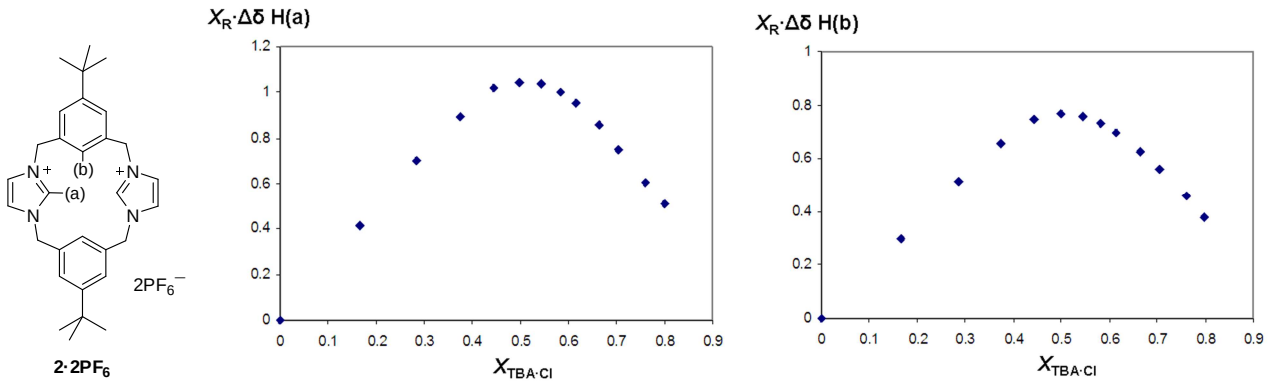

Figure S4. a) ^{1}H NMR (300MHz, 298K) spectra (low-field region) of receptor **2·2PF$_6$** in CD_3CN upon addition of increasing amounts of TBA·AcO (from bottom to top).
b) Job's plot representation from values of H(a) or H(b).

a)

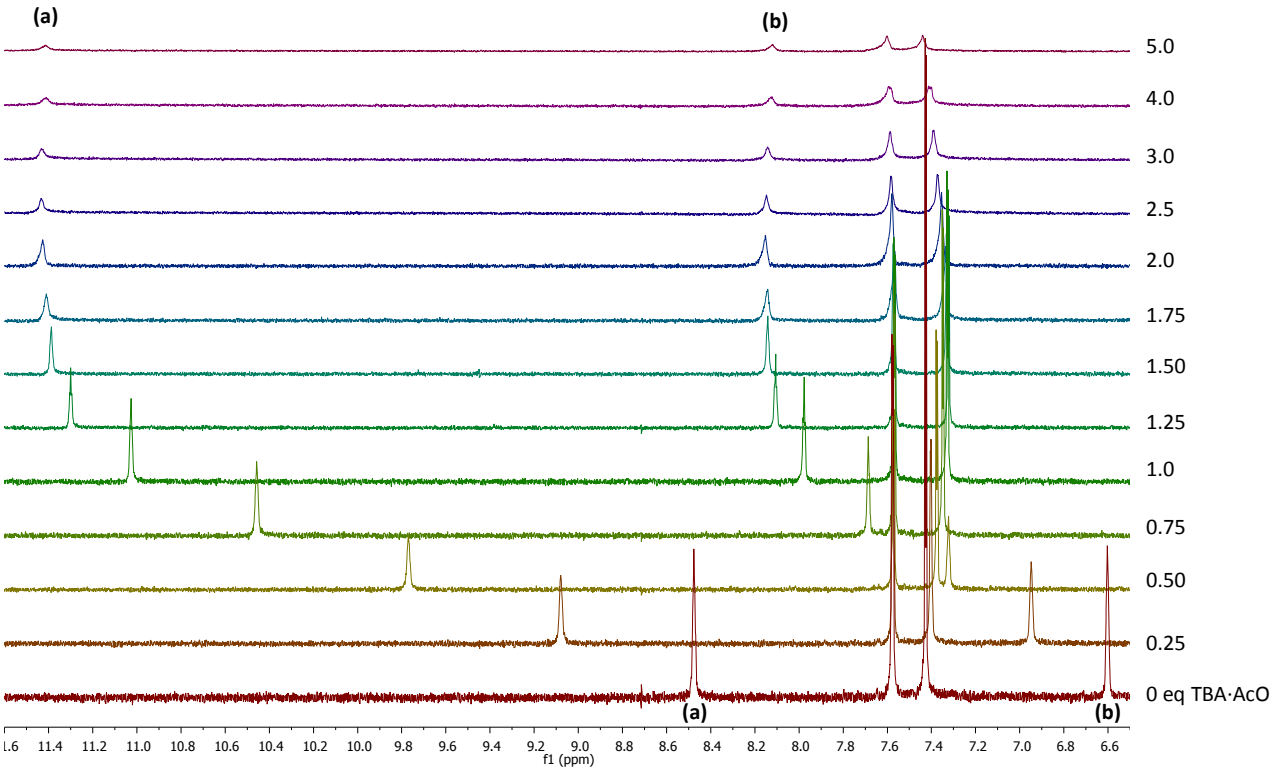

b)

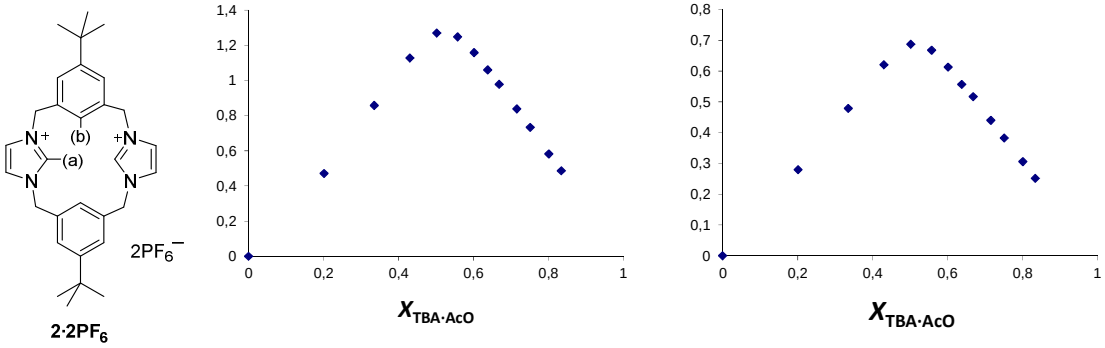

Figure S5. a) ^{1}H NMR (300MHz, 298K) spectra (low-field region) of receptor **2·2PF$_6$** in CD_3CN upon addition of increasing amounts of TBA·CN (from bottom to top).
b) Job's plot representation from values of H(a) or H(b).

a)

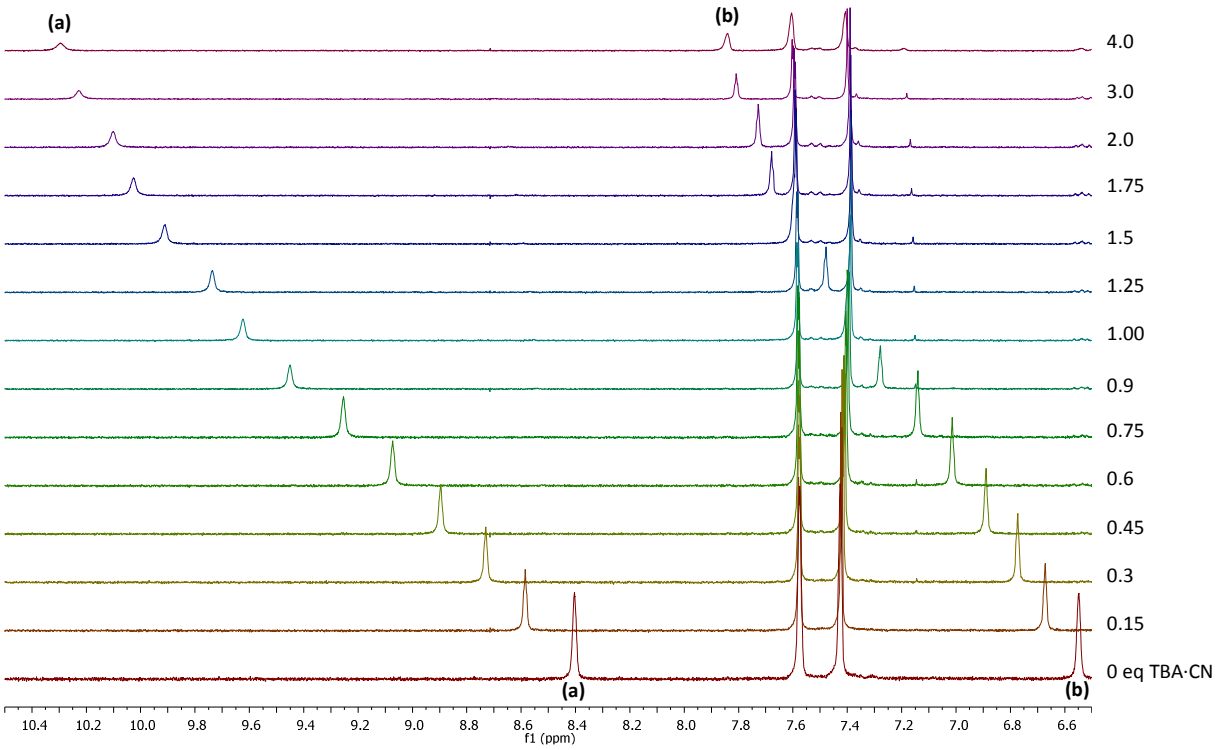

b)

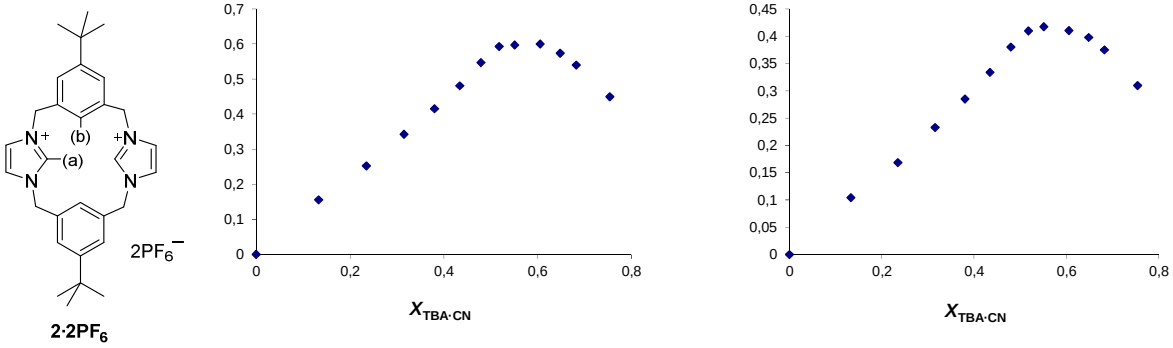

Figure S6. a) ^{1}H NMR (300MHz, 298K) spectra (low-field region) of receptor **4·2PF$_6$** in CD_3CN upon addition of increasing amounts of TBA·Cl (from bottom to top).

b) Job's plot representation from values of H(a) or H(b).

a)

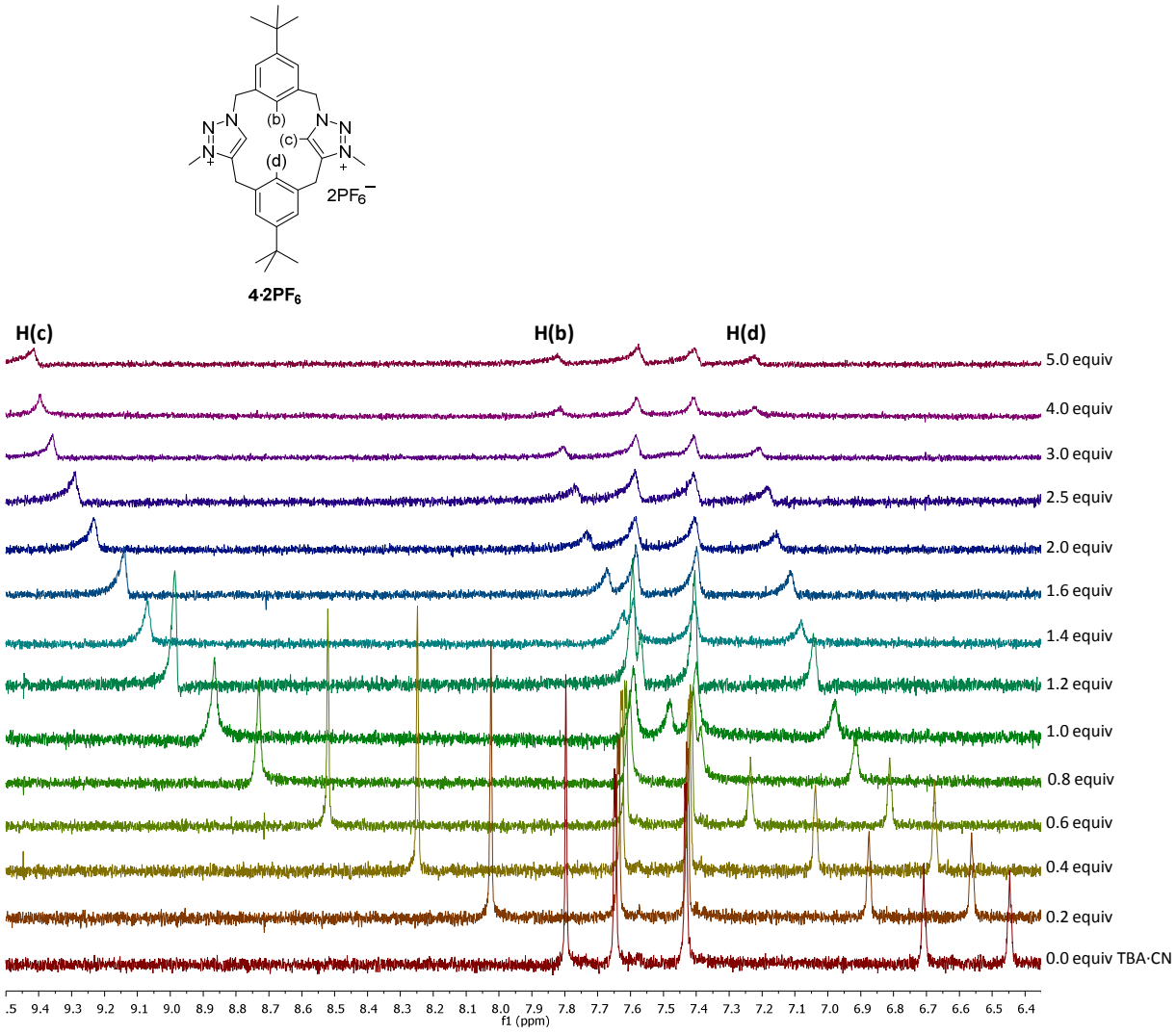

b)

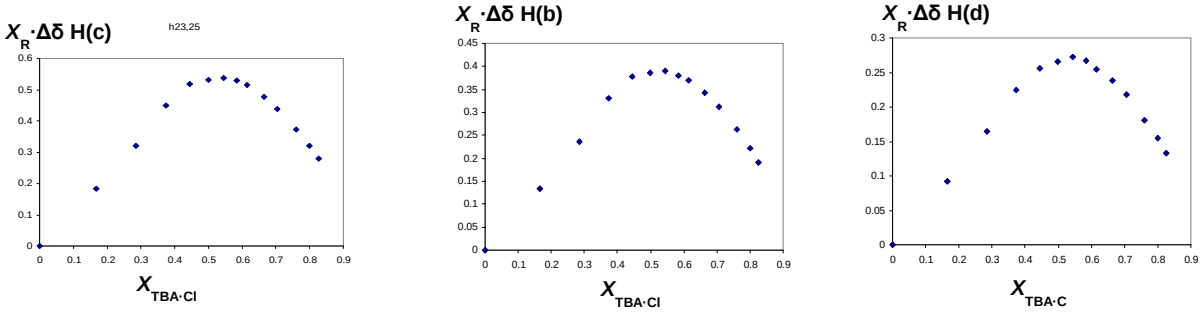

Figure S7. a) ^{1}H NMR (300MHz, 298K) spectra (low-field region) of receptor **4·2PF$_6$** in CD_3CN upon addition of increasing amounts of TBA·AcO (from bottom to top).

b) Job's plot representation from values of H(a) or H(b).

a)

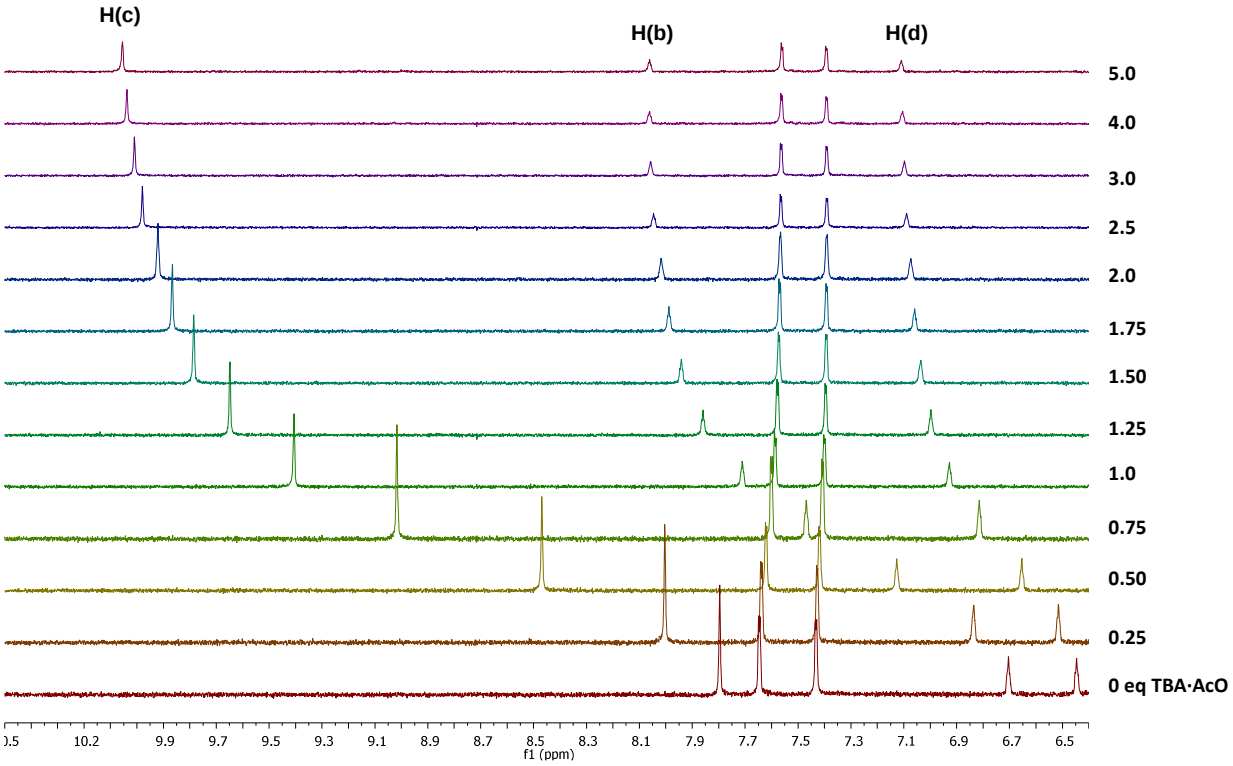

b)

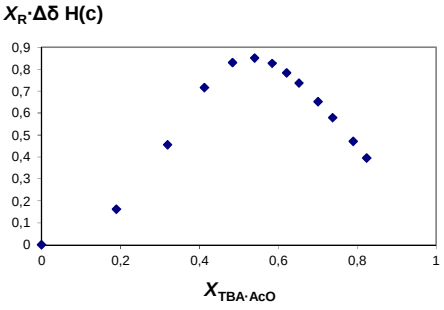

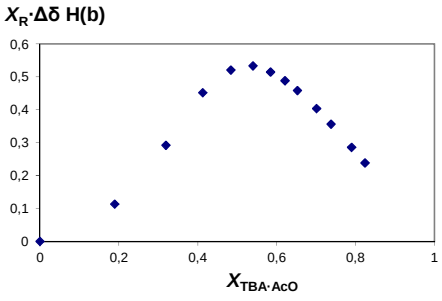

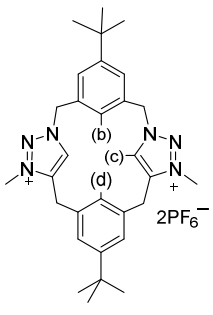

4·2PF$_6$

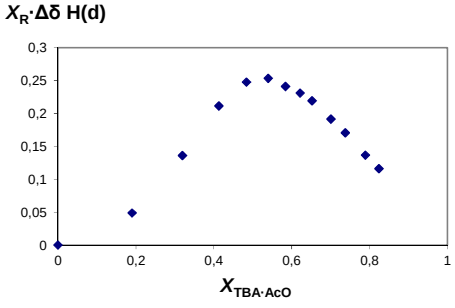

Figure S8. a) ^{1}H NMR (300MHz, 298K) spectra (low-field region) of receptor **4·2PF$_6$** in CD_3CN upon addition of increasing amounts of TBA·CN (from bottom to top).

b) Job's plot representation from values of H(a) or H(b).

a)

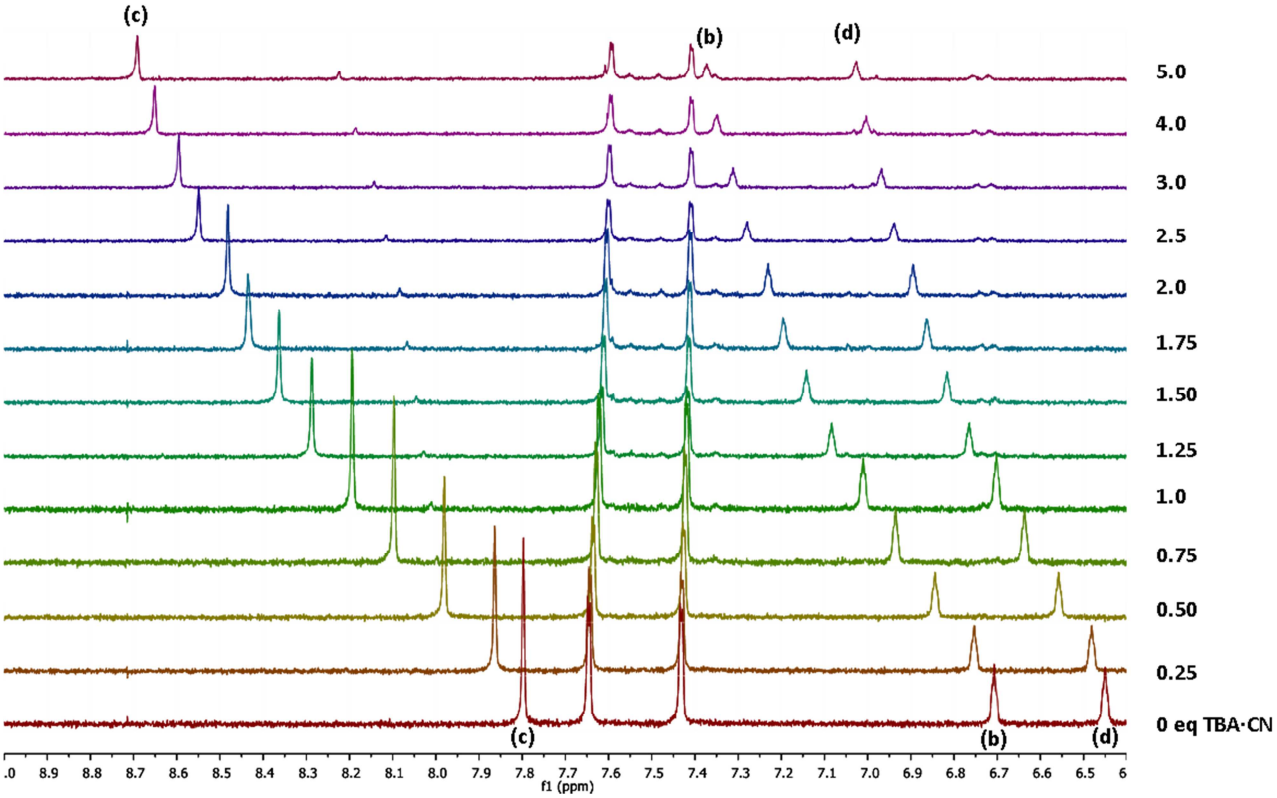

b) Isotherm could not be fitted to a 1:2 binding model.

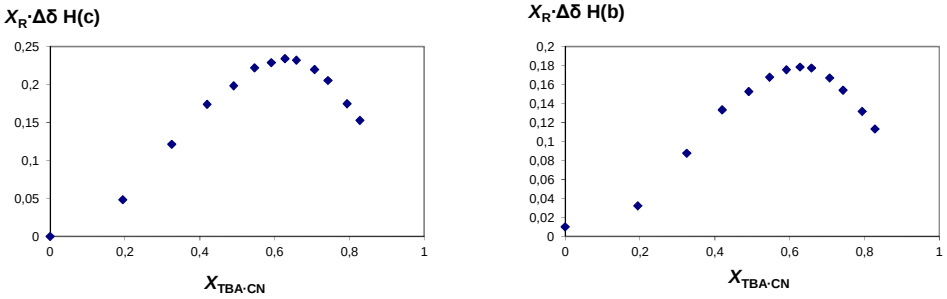

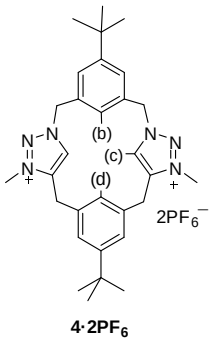

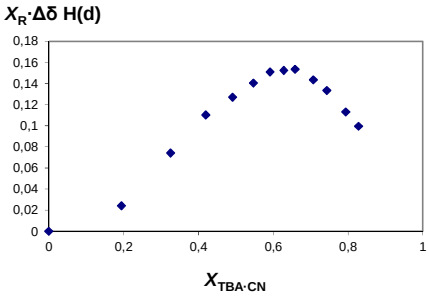

Figure S9. ^{1}H NMR (300MHz, 298K) spectra (low-field region) of receptor **2·2PF$_6$** in DMSO-d$_6$ upon addition of increasing amounts of TBA·Cl (from bottom to top).

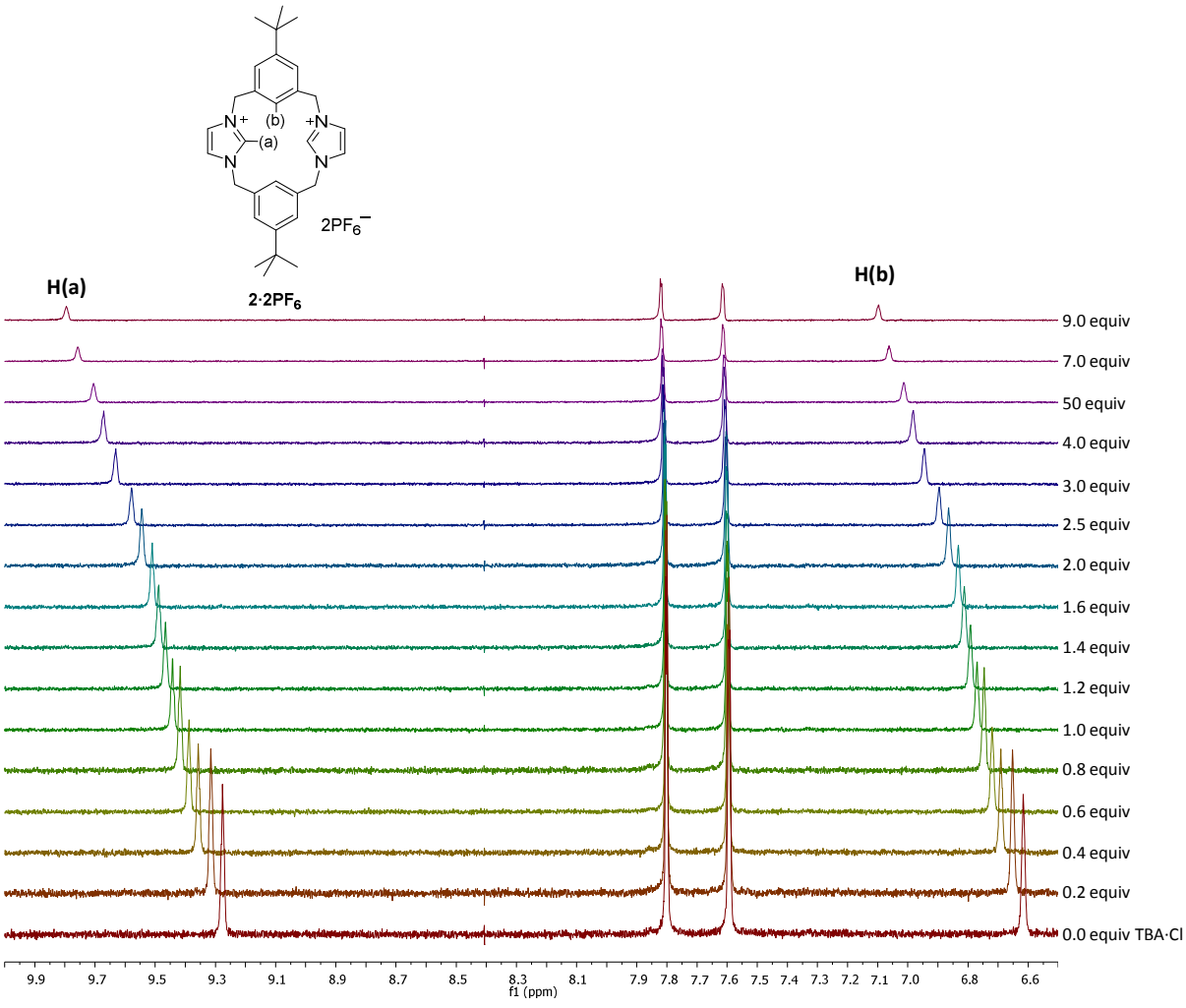

Figure S10. ^{1}H NMR (300MHz, 298K) spectra (low-field region) of receptor **2·2PF$_6$** in DMSO-d$_6$ upon addition of increasing amounts of TBA·AcO (from bottom to top).

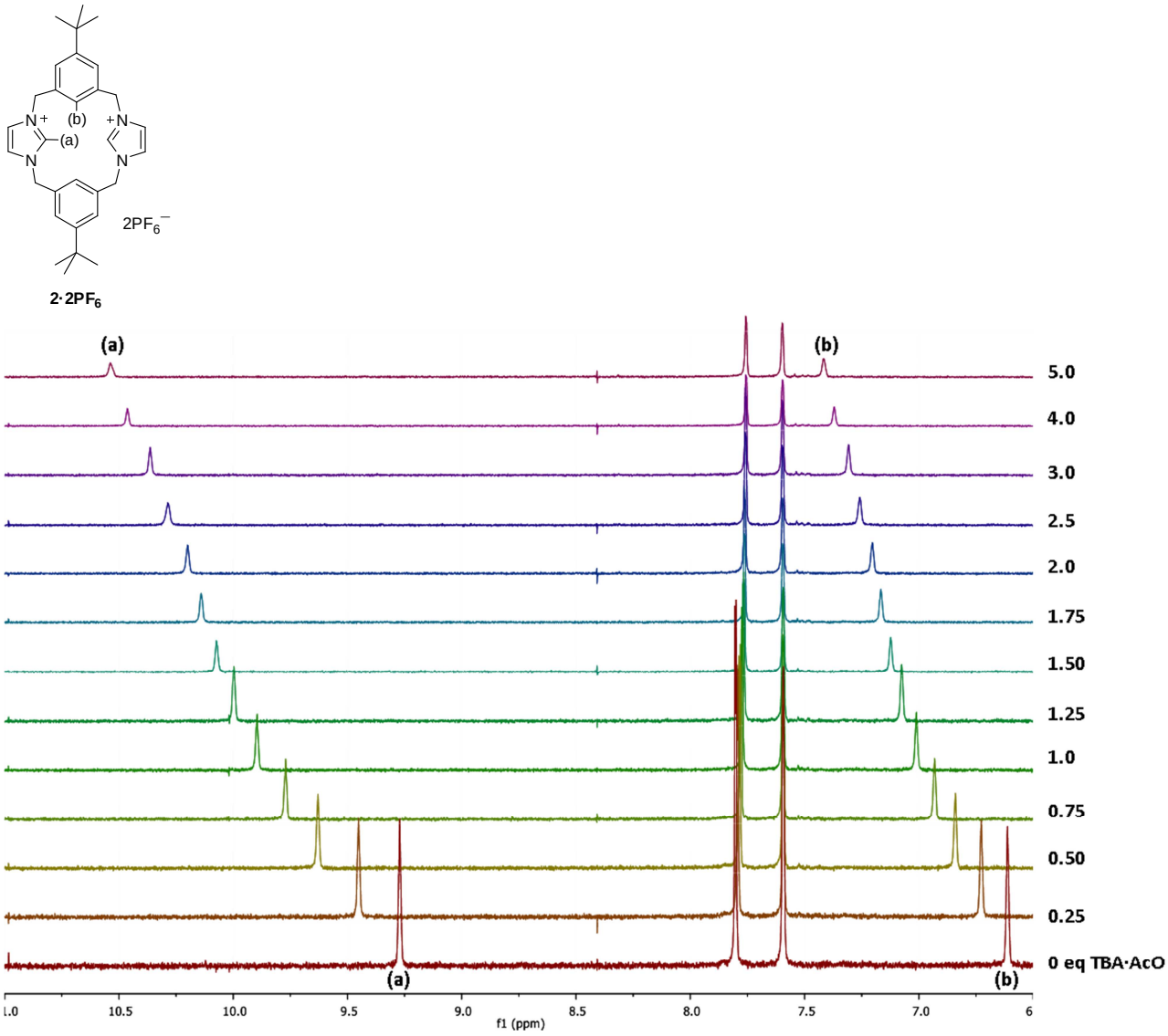

Figure S11. ^{1}H NMR (300MHz, 298K) spectra (low-field region) of receptor **2·2PF$_6$** in DMSO-d$_6$ upon addition of increasing amounts of TBA·H$_2$PO$_4$ (from bottom to top).

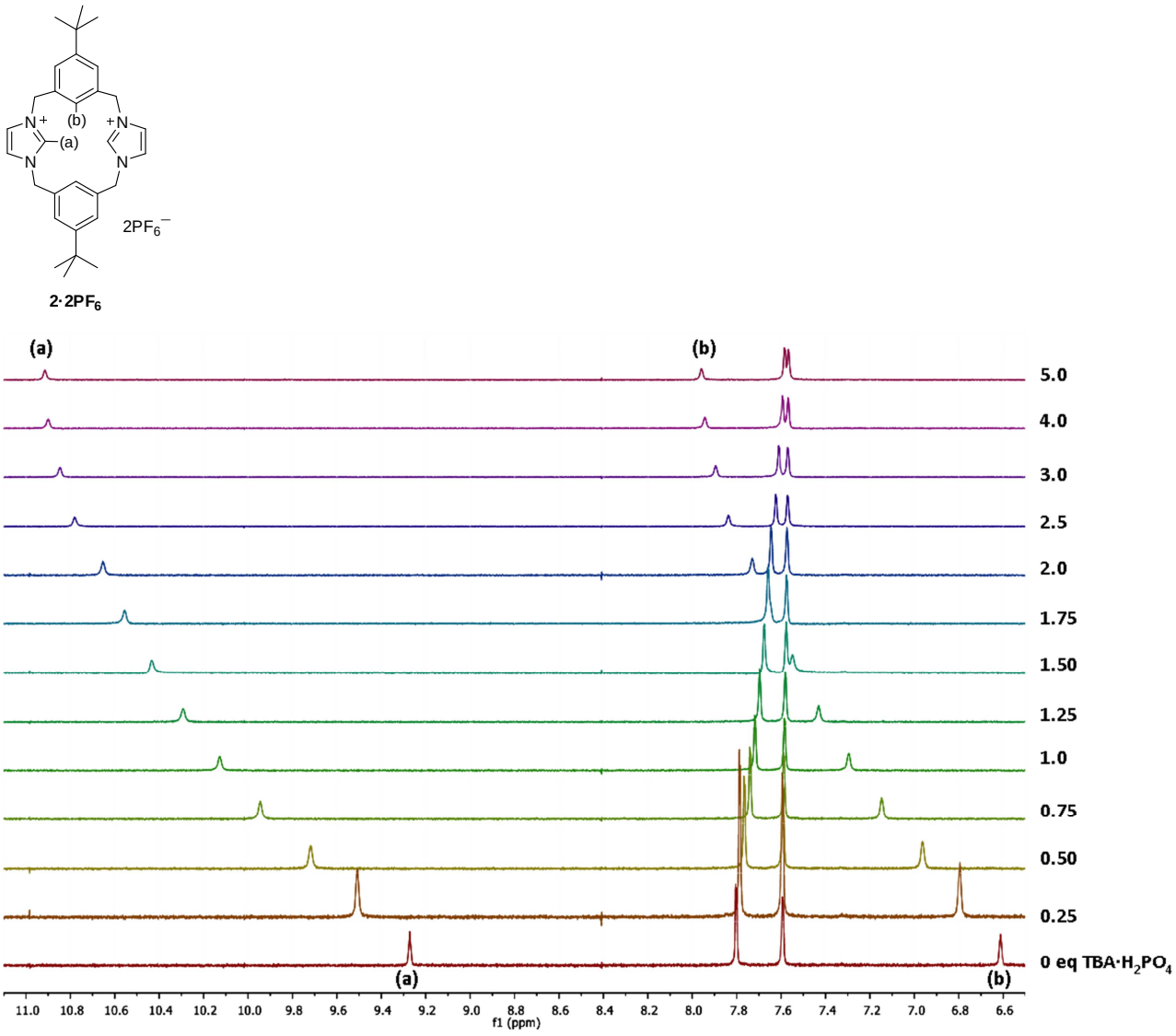

Figure S12. ^{1}H NMR (300MHz, 298K) spectra (low-field region) of receptor **2·2PF$_6$** in DMSO-d$_6$ upon addition of increasing amounts of TBA·CN (from bottom to top).

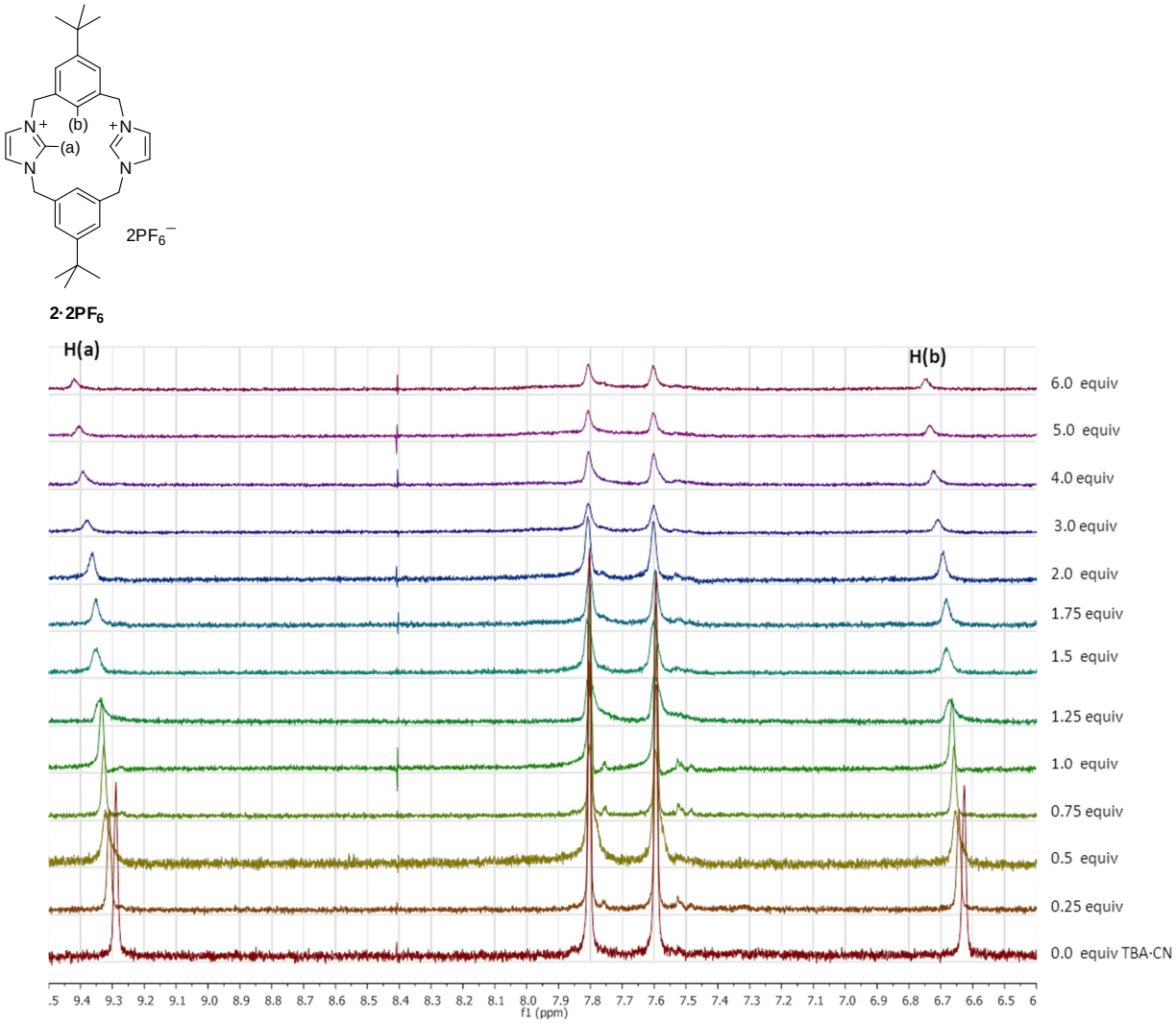

Figure S13. ^{1}H NMR (300MHz, 298K) spectra (low-field region) of receptor **4·2PF$_6$** in DMSO-d$_6$ upon addition of increasing amounts of TBA·Cl (from bottom to top).

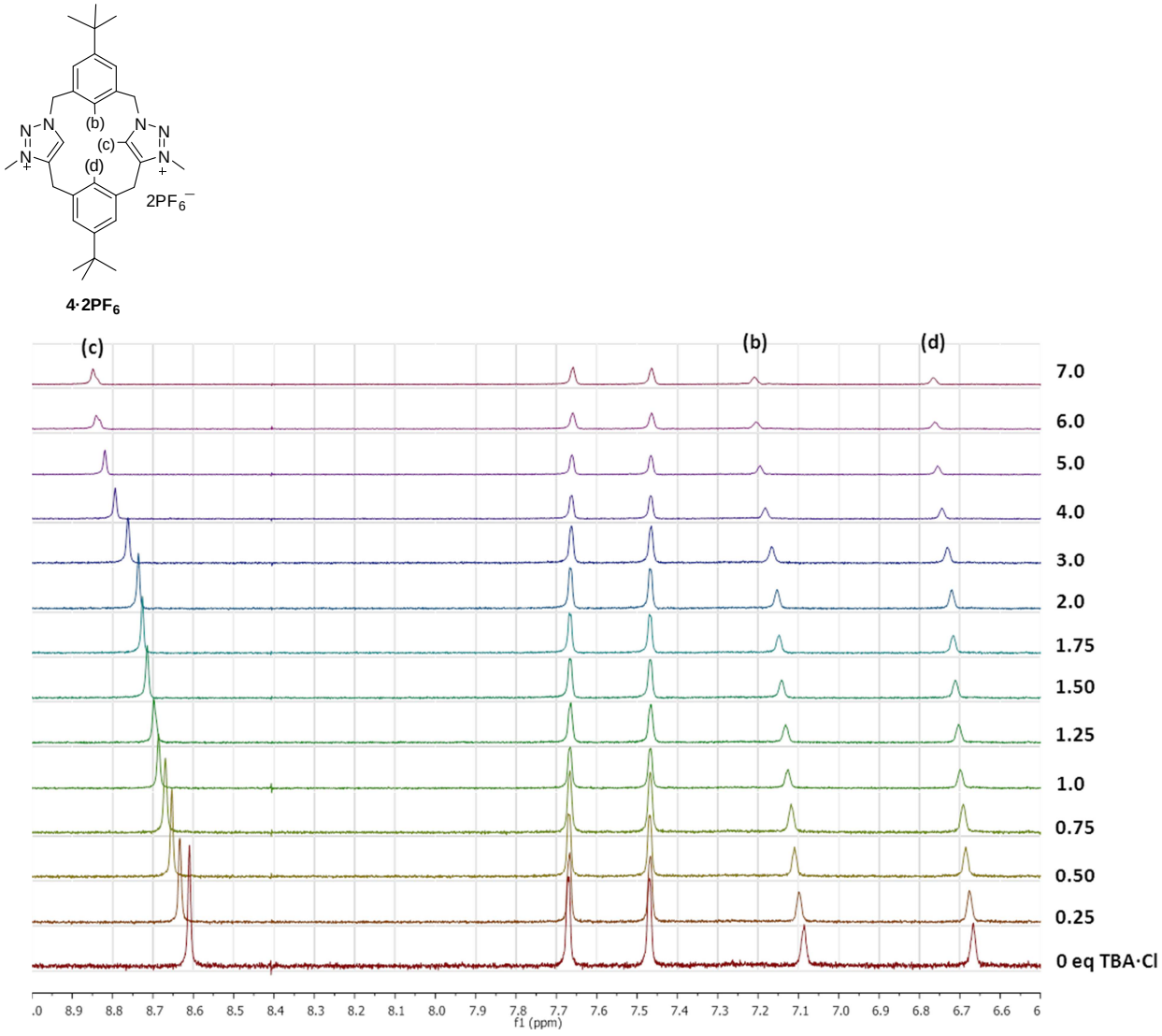

Figure S14. ^{1}H NMR (300MHz, 298K) spectra (low-field region) of receptor **4·2PF$_6$** in DMSO-d$_6$ upon addition of increasing amounts of TBA·AcO (from bottom to top).

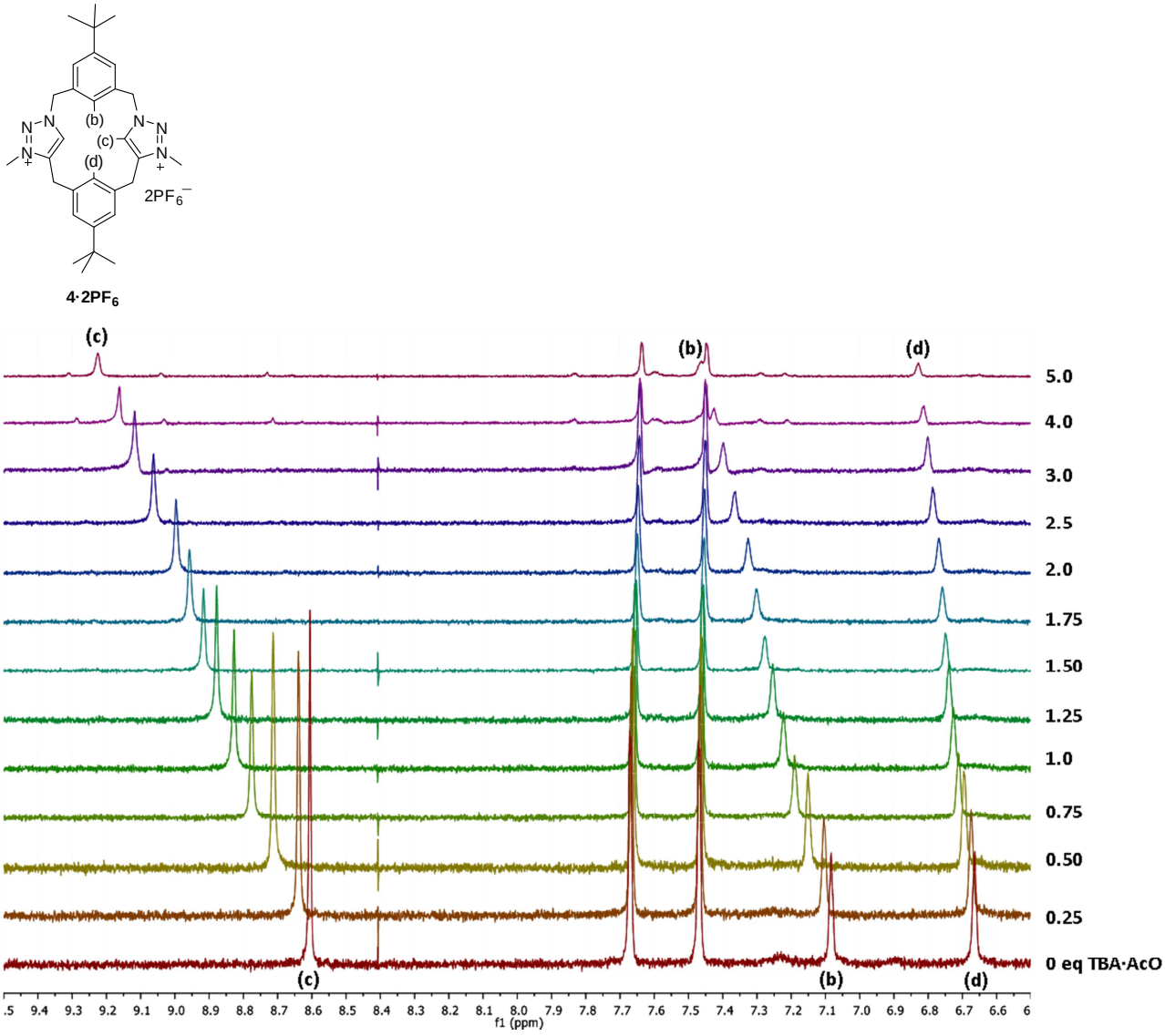

Figure S15. ^{1}H NMR (300MHz, 298K) spectra (low-field region) of receptor **4·2PF$_6$** in DMSO-d$_6$ upon addition of increasing amounts of TBA·H$_2$PO$_4$ (from bottom to top).

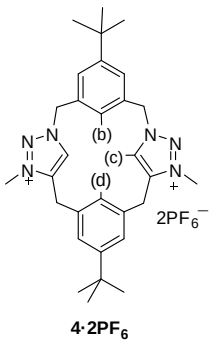

4·2PF$_6$

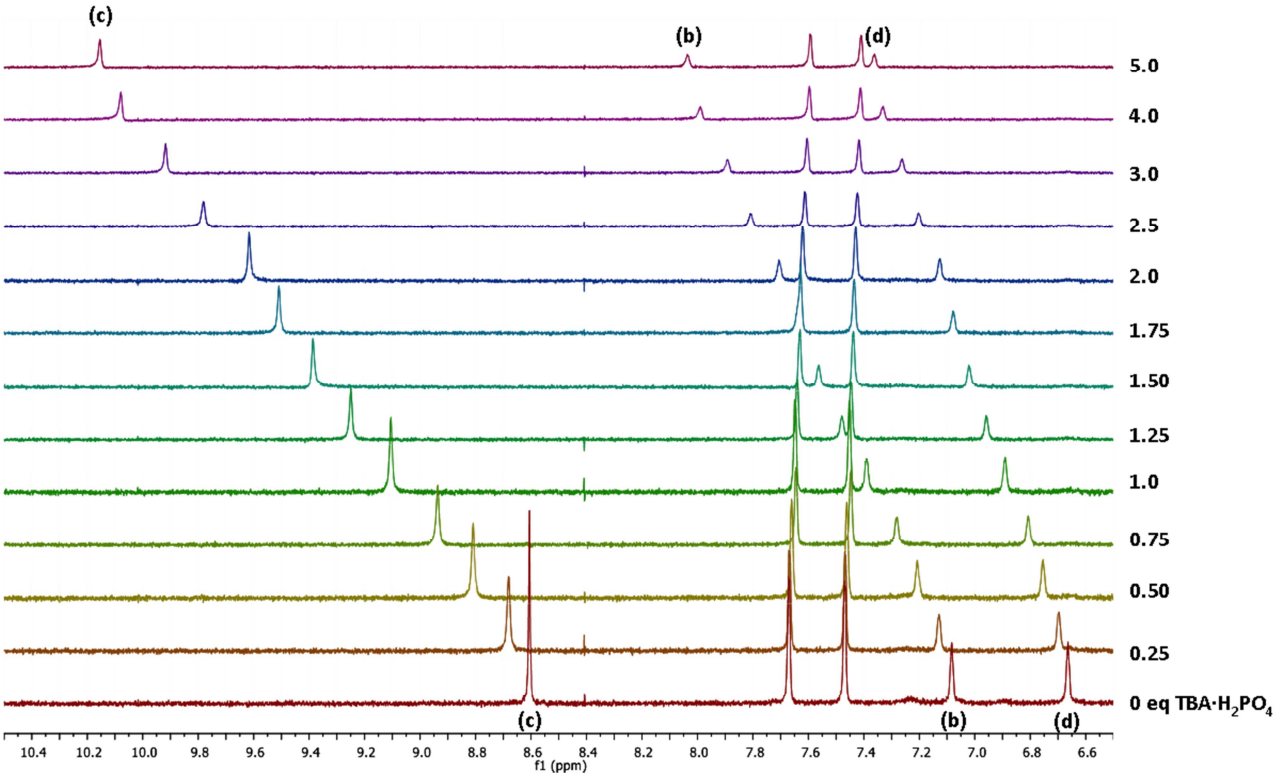

Figure S16. ^{1}H NMR (300MHz, 298K) spectra (low-field region) of receptor **4·2PF$_6$** in DMSO-d$_6$ upon addition of increasing amounts of TBA·CN (from bottom to top).

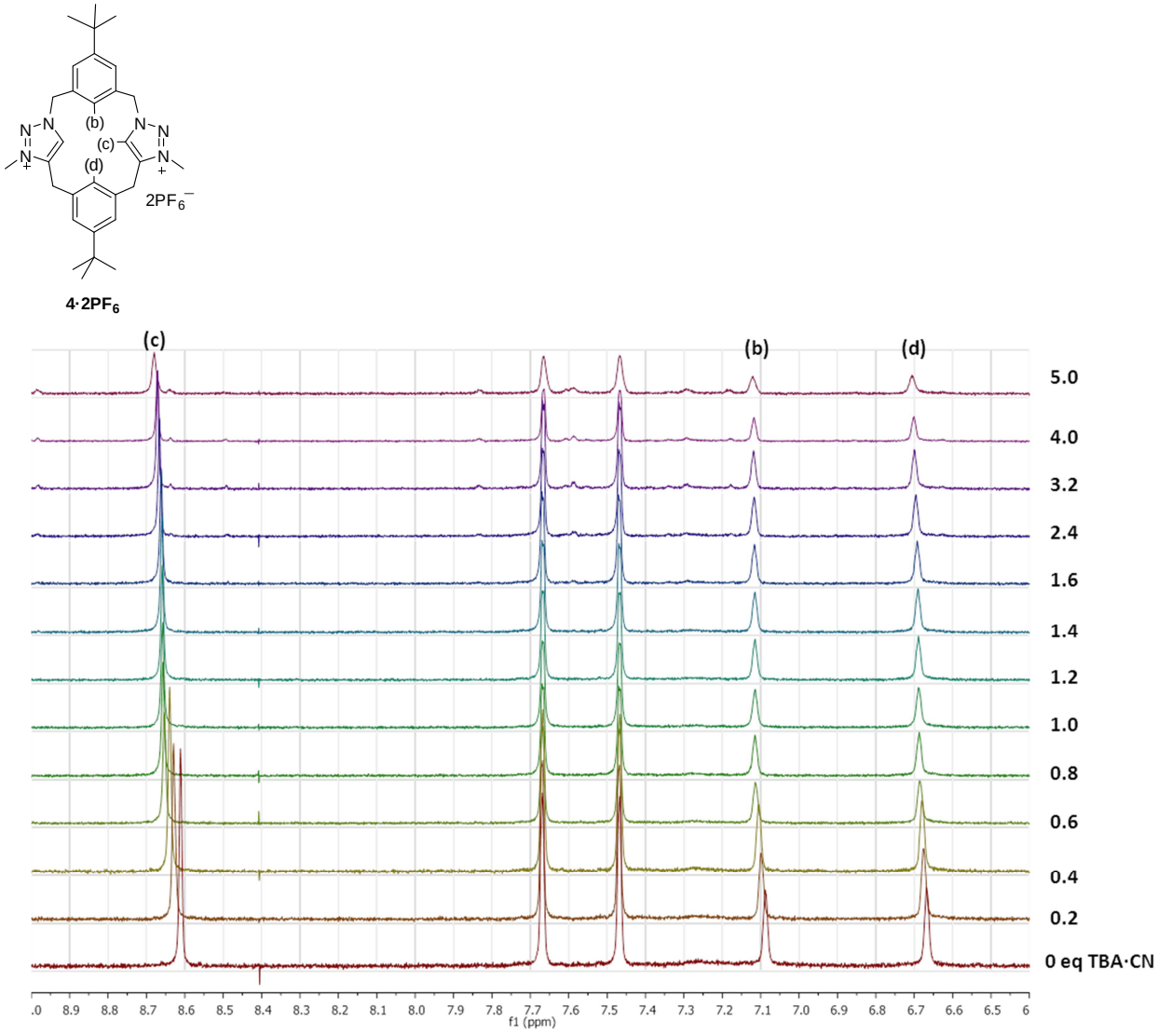

Figure S17. ^{1}H NMR (300MHz, 298K) spectra (low-field region) of receptor **5·PF$_6$** in CD_3CN upon addition of increasing amounts of TBA·Cl (from bottom to top).

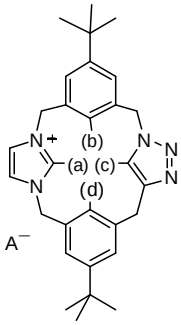

5·A

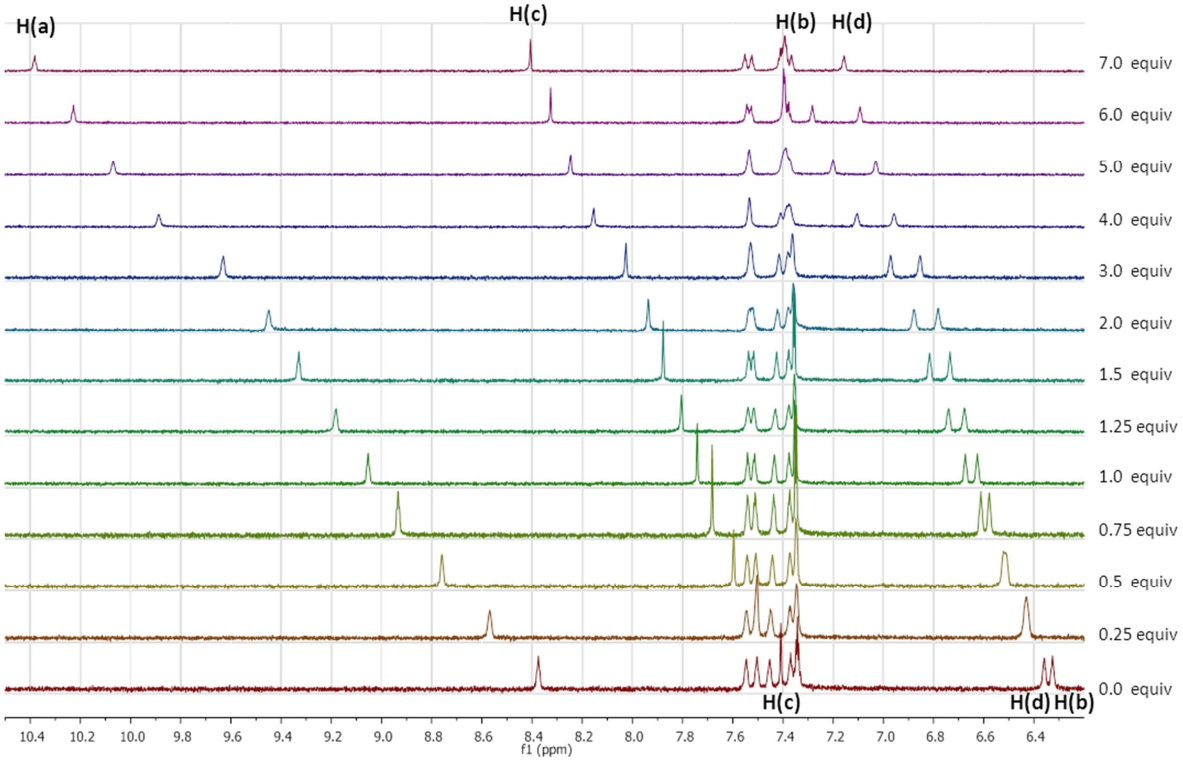

Figure S18. ^{1}H NMR (300MHz, 298K) spectra (low-field region) of receptor **5·PF$_6$** in CD_3CN upon addition of increasing amounts of TBA·AcO (from bottom to top).

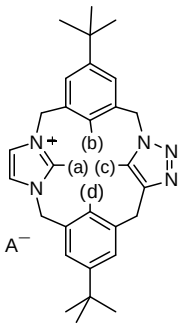

5·A

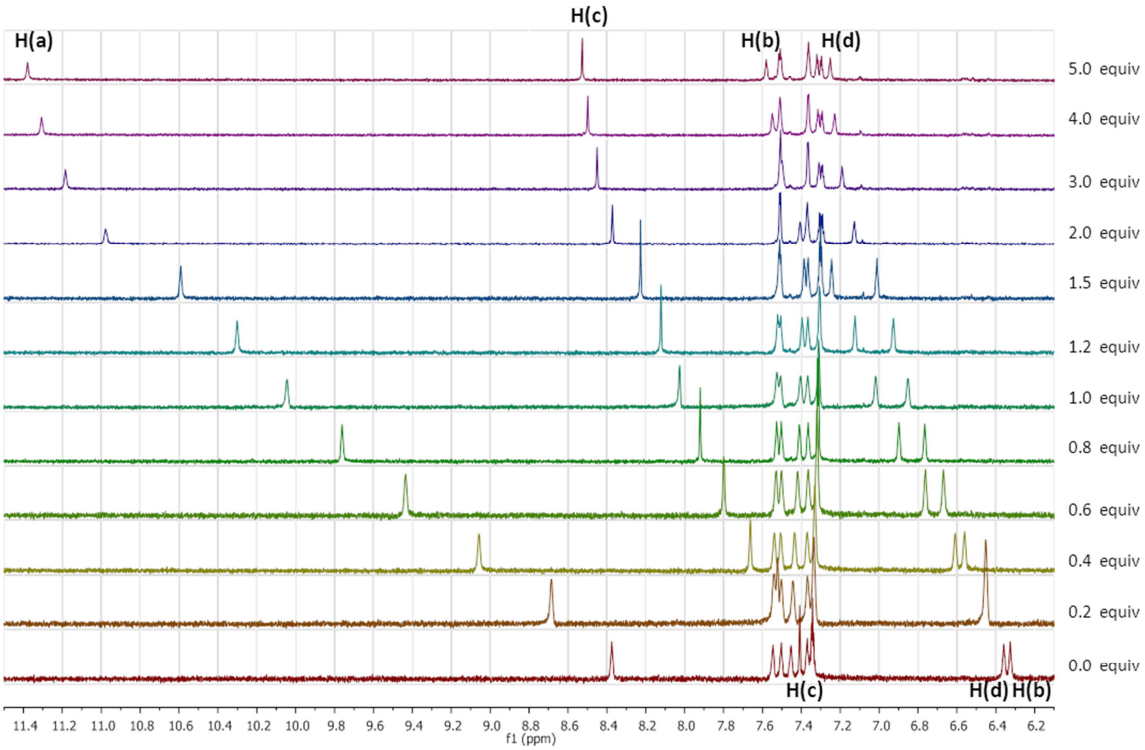

Figure S19. ^{1}H NMR (300MHz, 298K) spectra (low-field region) of receptor **5·PF$_6$** in CD_3CN upon addition of increasing amounts of TBA·H_2PO_4 (from bottom to top).

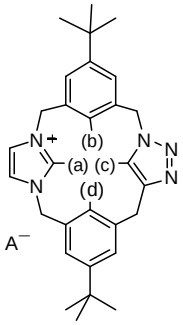

5·A

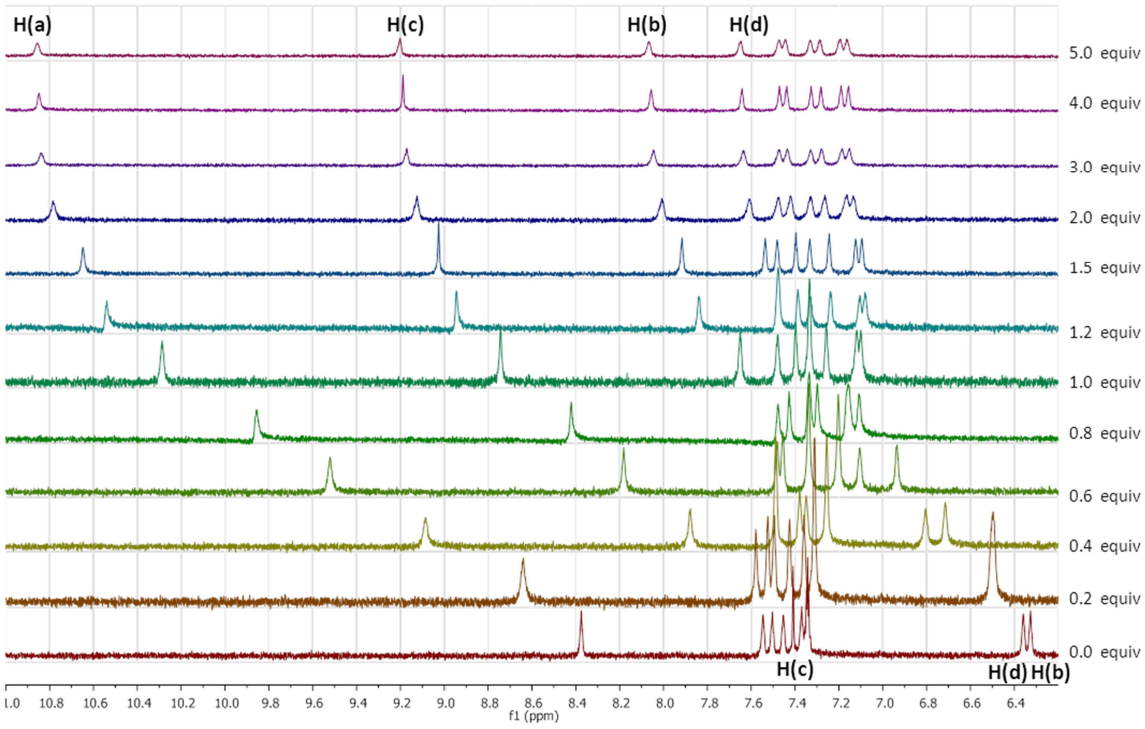

Figure S20. ^{1}H NMR (300MHz, 298K) spectra (low-field region) of receptor **5·PF$_6$** in CD_3CN upon addition of increasing amounts of TBA·CN (from bottom to top).

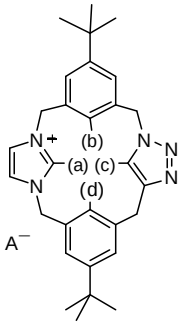

5·A

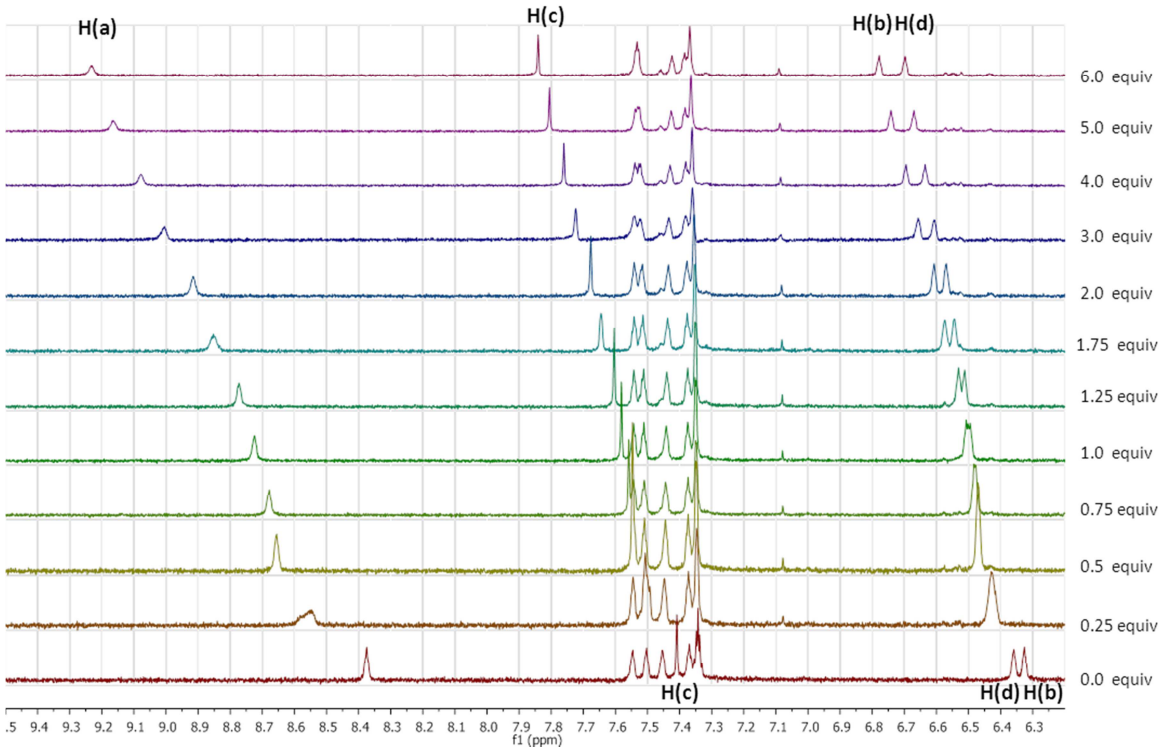

Figure S21. ^{1}H NMR (300MHz, 298K) spectra (low-field region) of receptor **5·PF$_6$** in DMSO-d$_6$ upon addition of increasing amounts of TBA·AcO (from bottom to top).

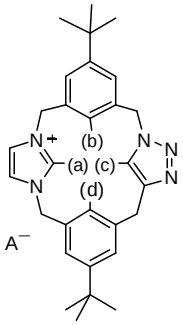

5·A

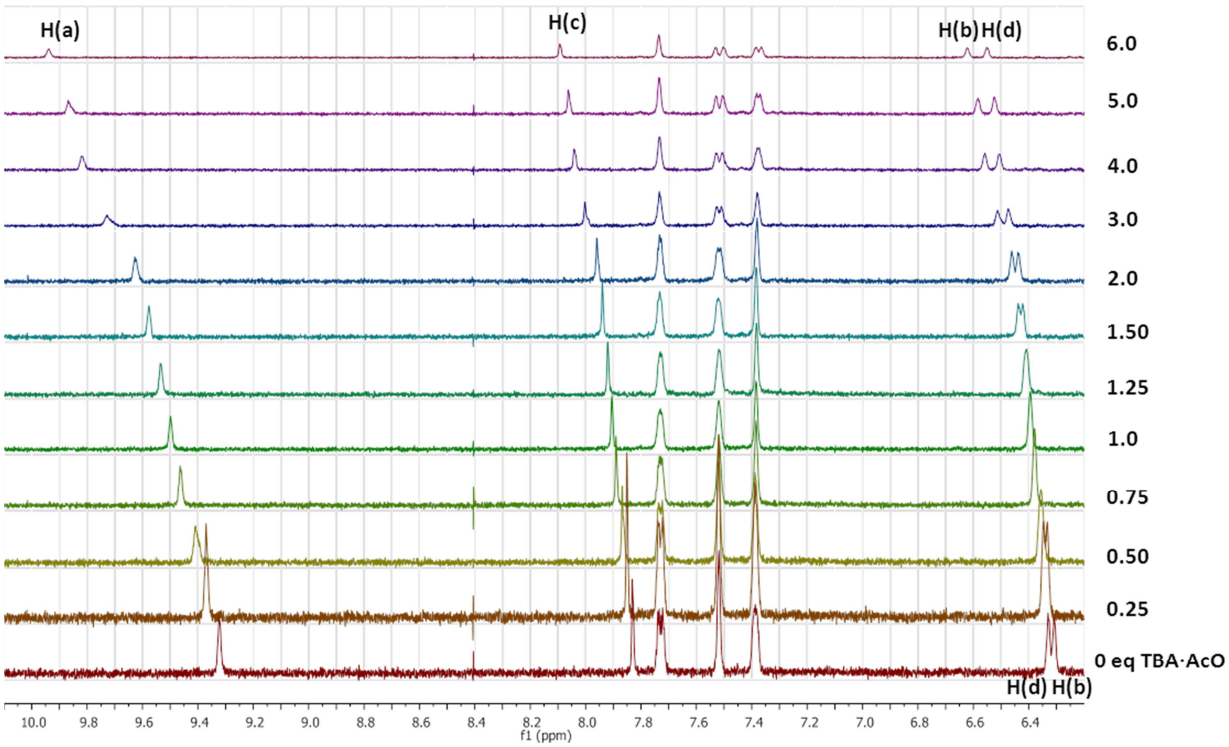

Figure S22. ^{1}H NMR (300MHz, 298K) spectra (low-field region) of receptor **5·PF$_6$** in DMSO-d$_6$ upon addition of increasing amounts of TBA·H$_2$PO$_4$ (from bottom to top).

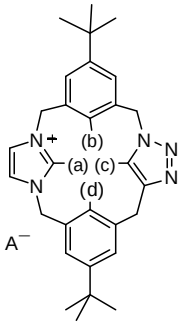

5·A

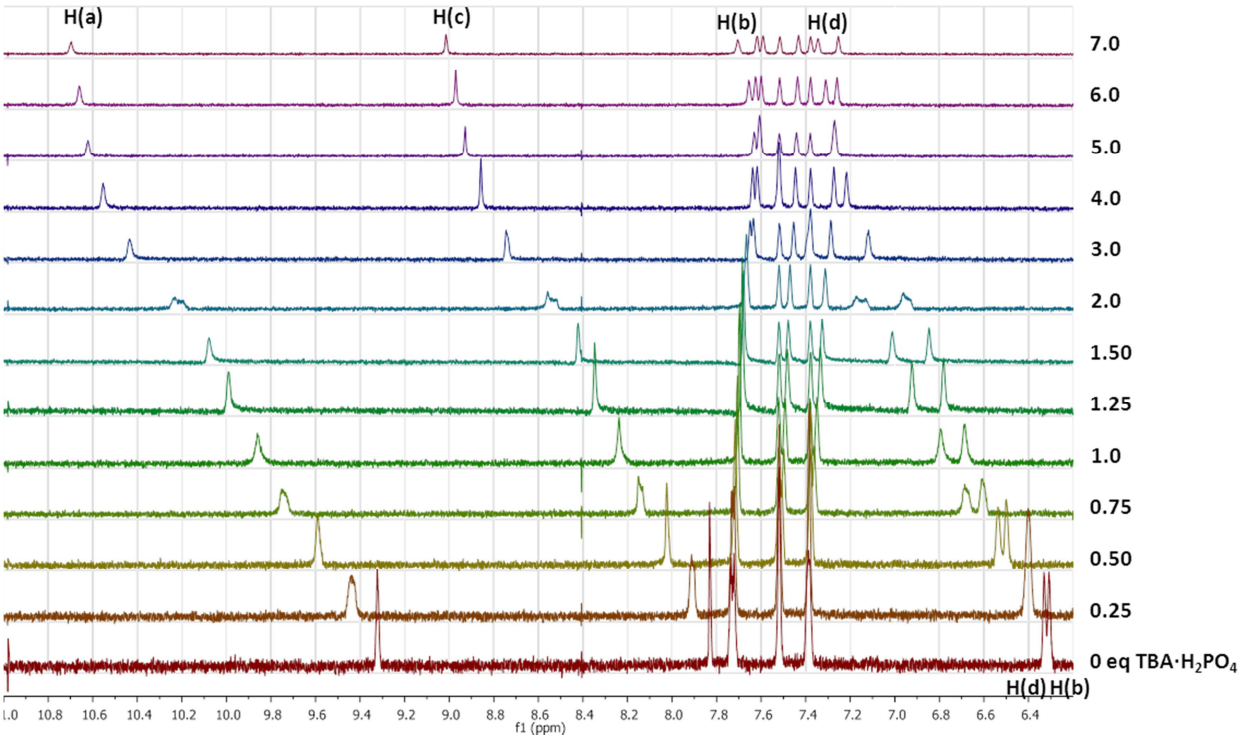

Figure S23. ^{1}H NMR titration curves of the receptor **2·2PF$_6$** (initial host concentration ca. 3 mM in CD_3CN, 300 MHz) with corresponding TBA salts represented from values of H(a) or H(b).

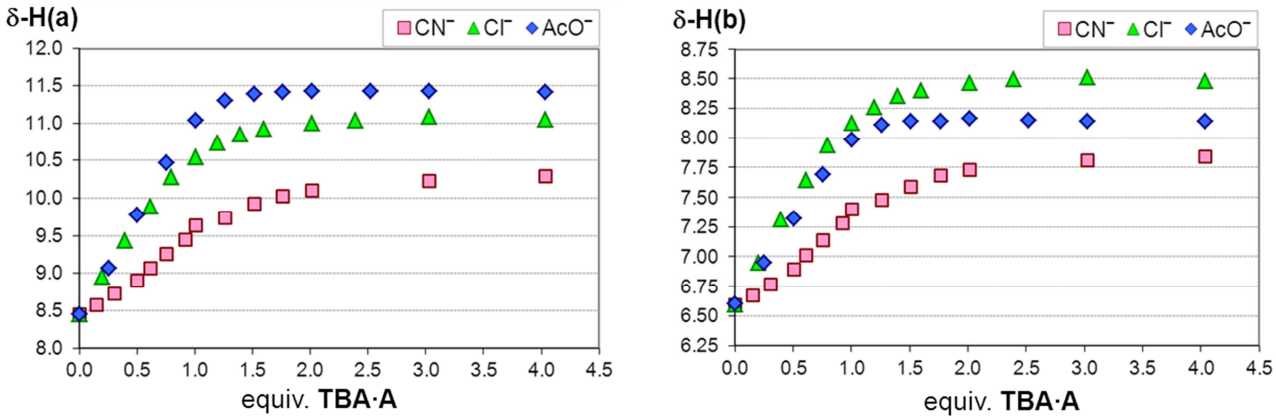

Figure S24. ^{1}H NMR titration curves of the receptor **2·2PF$_6$** (initial host concentration ca. 3 mM in DMSO-d_6, 300 MHz) with corresponding TBA salts represented from values of H(a) or H(b).

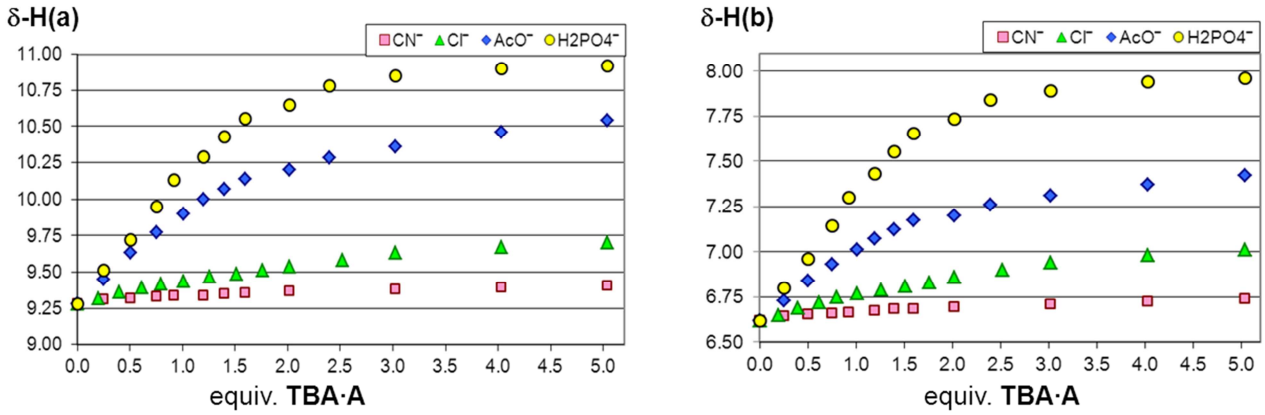

Figure S25. ^{1}H NMR titration curves of the receptor **4·2PF$_6$** (initial host concentration ca. 3 mM in CD_3CN, 300 MHz) with corresponding TBA salts represented from values of H(c), H(b) or H(d).

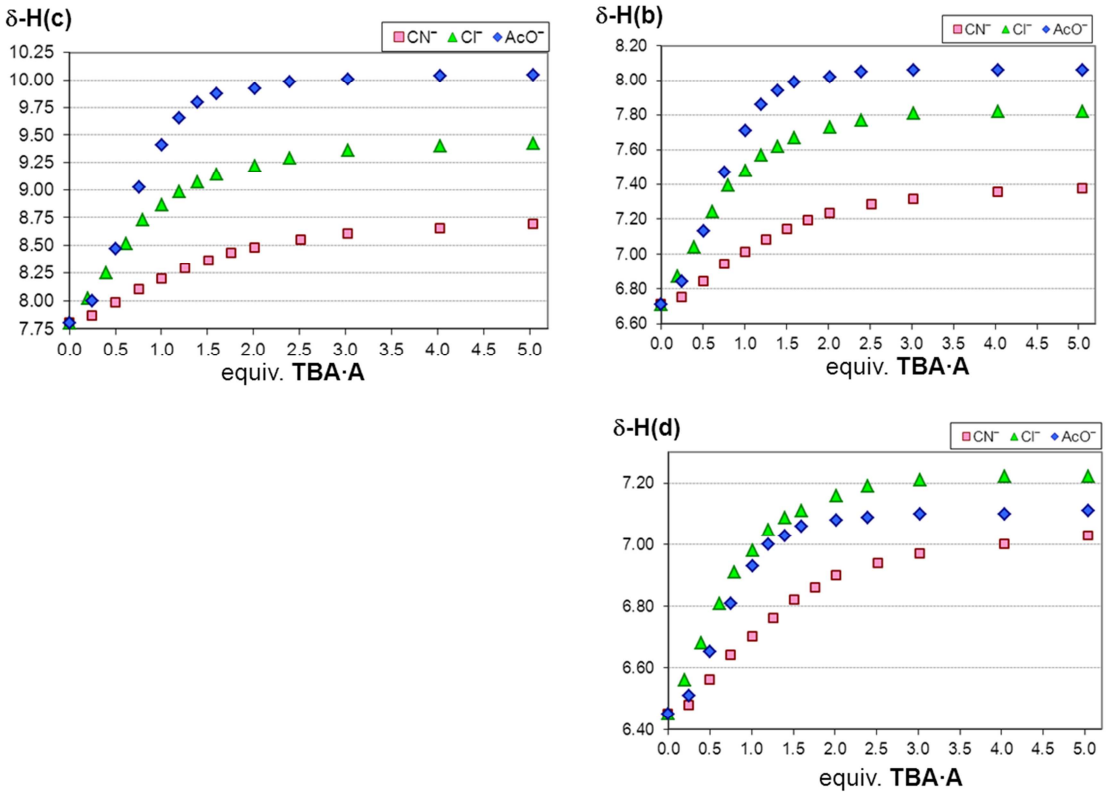

Figure S26. ^{1}H NMR titration curves of the receptor **4·2PF$_6$** (initial host concentration ca. 3 mM in DMSO-d_6, 300 MHz) with corresponding TBA salts represented from values of H(c), H(b) or H(d).

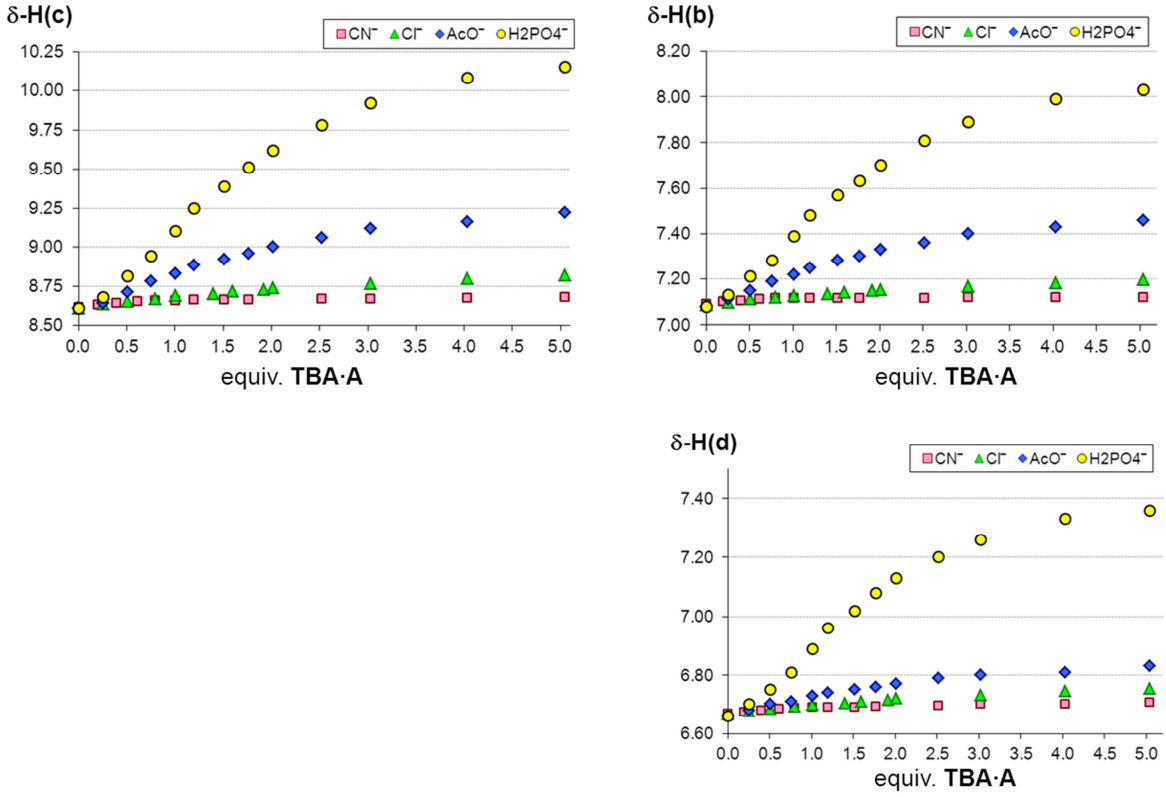

Figure S27. ^{1}H NMR titration curves of the receptor **5·PF$_6$** (initial host concentration ca. 3 mM in CD_3CN, 300 MHz) with corresponding TBA salts represented from values of H(a), H(b), H(c) or H(d).

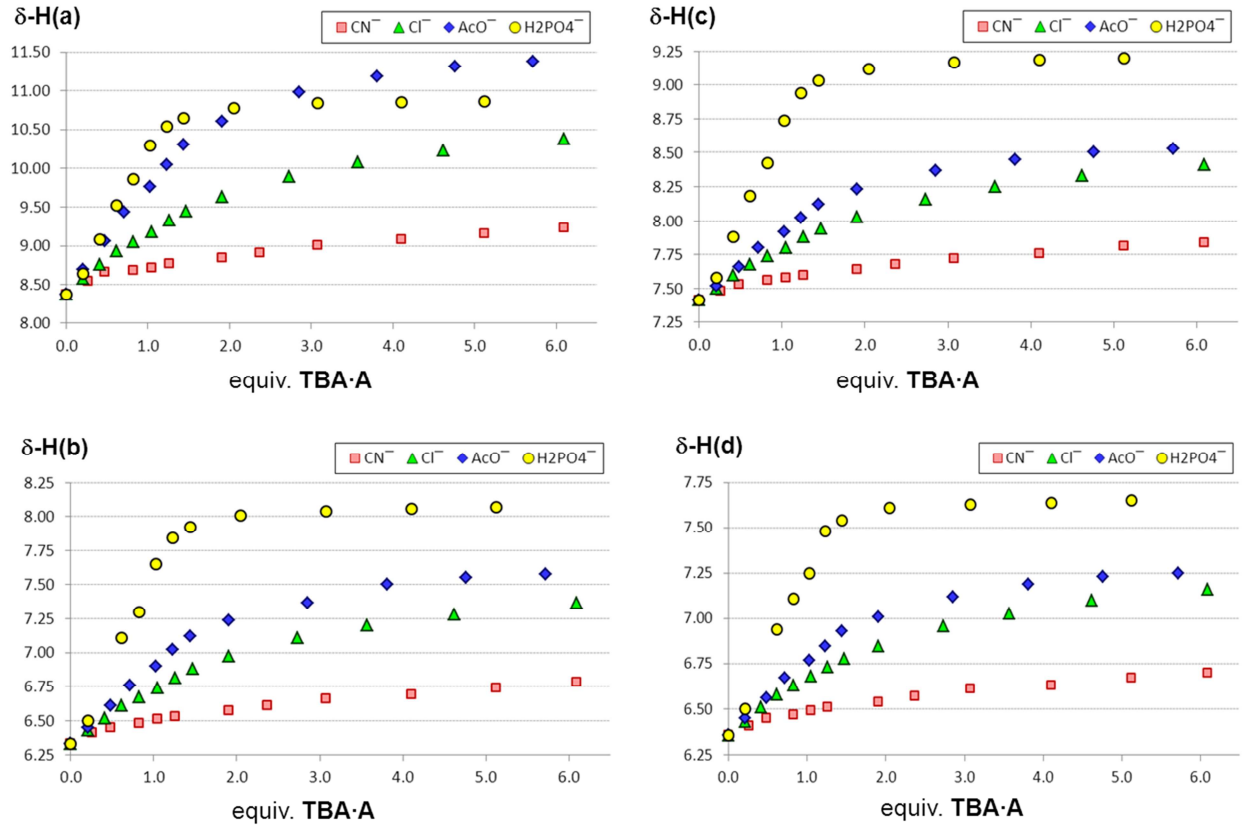

Figure S28. ^{1}H NMR titration curves of the receptor **5·PF$_6$** (initial host concentration ca. 3 mM in DMSO-d_6, 300 MHz) with corresponding TBA salts represented from values of H(a), H(b), H(c) or H(d).

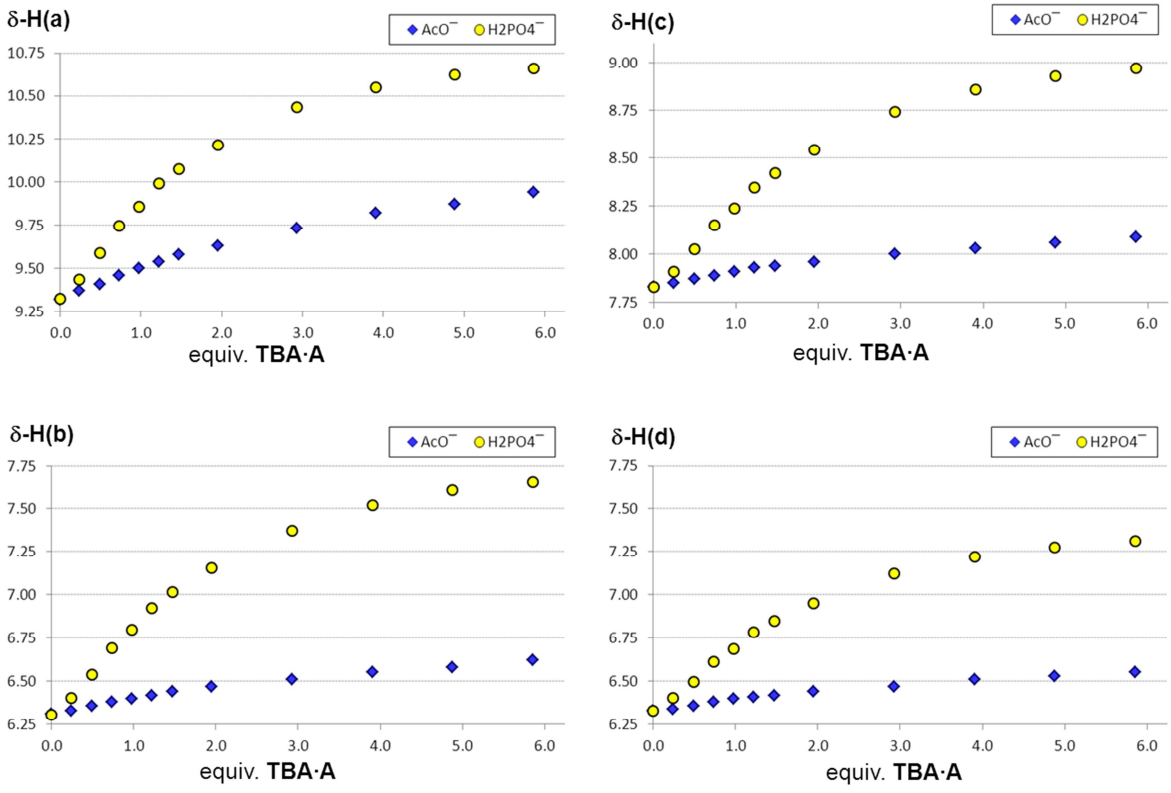

Table S3. Association constants for each shifted hydrogen atom K_a (M^{-1}) and free energies $-\Delta G°$ ($kJ \cdot mol^{-1}$) for compounds **2·2PF$_6$**, **4·2PF$_6$** or **5·PF$_6$** and various anions at 298 K in CD_3CN and DMSO-d_6.[a]

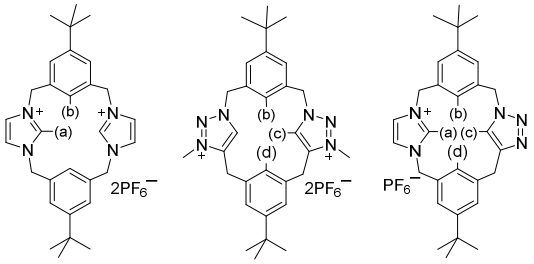

2·2PF$_6$ **4·2PF$_6$** **5·PF$_6$**

CD_3CN

Anion	Stoichiometry complex	H(a)		H(b)		H(c)		H(d)	
2·2PF$_6$		K_a	$-\Delta G°$	K_a	$-\Delta G°$	K_a	$-\Delta G°$	K_a	$-\Delta G°$
Cl^-	1:1	5053±70	21.13	4838±132	21.02	—	—	—	—
AcO^-	1:1	8640±562	22.46	9508±562	22.70	—	—	—	—
CN^-	1:1	1148±113	17.47	1251±113	17.68	—	—	—	—
4·2PF$_6$									
Cl^-	1:1	—	—	2101±114	18.95	1585±84	18.26	2146±70	19.01
AcO^-	1:1	—	—	5864±209	21.50	4580±176	20.89	3952±131	20.52
CN^-	1:1	—	—	472±5[b]	15.26	745±57	16.39	787±80	16.52
5·PF$_6$									
Cl^-	1:1	166±15	12.67	190±11	13.00	195±13	13.06	189±9	12.99
AcO^-	1:1	509±30	15.44	477±37	15.28	492±27	15.36	502±33	15.41
$H_2PO_4^-$	1:1	4780±442	20.99	4531±526[c]	20.86	3553±412[c]	20.26	3164±386[c]	19.97
CN^-	1:1	95±11[b]	11.28	78±11[d]	10.79	84±12[d]	10.98	102±16[e]	11.46

DMSO-d_6

Anion	Stoichiometry complex	H(a)		H(b)		H(c)		H(d)	
2·2PF$_6$		K_a	$-\Delta G°$	K_a	$-\Delta G°$	K_a	$-\Delta G°$	K_a	$-\Delta G°$
Cl^-	1:1[f]	87±5	11.06	92±6	11.20	—	—	—	—
AcO^-	1:1[f]	548±44	15.63	371±16	14.66	—	—	—	—
CN^-	1:1[f]	63±7[b]	10.27	108±2	11.60	—	—	—	—
$H_2PO_4^-$	1:1[f]	670±83[c]	16.12	664±93[c]	16.10	—	—	—	—
4·2PF$_6$									
Cl^-	1:1[f]	—	—	67±4	10.41	56±3	9.97	64±4	10.30
AcO^-	1:1[f]	—	—	176±12	12.81	191±11	13.01	313±1	14.24
$H_2PO_4^-$	1:1[f]	—	—	218±4	13.34	245±35[d]	13.63	282±38[g]	13.98
5·PF$_6$									
AcO^-	1:1	74±6	10.66	76±11[d]	10.73	72±8[b]	10.60	76±8	10.73
$H_2PO_4^-$	1:1	263±14	13.81	197±10	13.09	193±12	13.04	208±14	13.22

[a]Error ≤ 10% except where noted. [b]Error 11%. [c]Error 12%. [d]Error 14%. [e]Error 16%. [f]Stoichiometric binding model in which the error is lower. [g] Error 13%.

Table S4. Average association constants K_a (M^{-1}) and free energies $-\Delta G°$ ($kJ \cdot mol^{-1}$) for compounds **2·2PF$_6$**, **4·2PF$_6$** or **5·PF$_6$** and various anions at 298 K in CD_3CN and DMSO-d_6[a]

Anion	CD_3CN			DMSO-d_6		
2·2PF$_6$	Stoichiometry complex	K_a	$-\Delta G°$	Stoichiometry complex	K_a	$-\Delta G°$[b]
Cl^-	1:1	4946	21.08	1:1	90	11.13
AcO^-	1:1	9074	22.58	1:1	460	15.15
CN^-	1:1	1200	17.57	1:1	86	10.94
$H_2PO_4^-$	*b*			1:1	667[c]	16.11
4·2PF$_6$						
Cl^-	1:1	1944	18.74	1:1	62	10.23
AcO^-	1:1	4799	20.97	1:1	227	13.35
CN^-	1:1	668	16.06	*d*		
$H_2PO_4^-$	*b*			1:1	248	13.65
5·PF$_6$						
Cl^-	1:1	185	12.93		n.d.	
AcO^-	1:1	495	15.37	1:1	75	10.68
CN^-	1:1	90[e]	11.13		n.d.	
$H_2PO_4^-$	1:1	4007[f]	20.52	1:1	215	13.31

n.d: not determined. [a]Average association constants from each shifted hydrogen atom. Average errors ≤ 10% except where noted. [b]Precipitation ocurred during titriation. [c]Average error 12%. [d]If after additon of a large excess of the anion $\Delta\delta \leq 0.1$ ppm, data were not processed. [e]Average error 14%. [f]Average error 11%.